การผลิตไฮโดรเจนผ่านปฏิกิริยารีฟอร์มมิงแก๊สชีวภาพด้วยไอน้ำที่ส่งเสริมด้วยการดูดซับ

โดยใช้นิกเกิลเป็นตัวเร่งปฏิกิริยา

นายเจนวิทย์ พรหมประสิทธิ์

วิทยานิพนธ์นี้เป็นส่วนหนึ่งของการศึกษาตามหลักสูตรปริญญาวิศวกรรมศาสตรมหาบัณฑิต

สาขาวิชาวิศวกรรมเคมี ภาควิชาวิศวกรรมเคมี

คณะวิศวกรรมศาสตร์ จุฬาลงกรณ์มหาวิทยาลัย

ปีการศึกษา 2554

ลิขสิทธิ์ของจุฬาลงกรณ์มหาวิทยาลัย

HYDROGEN PRODUCTION VIA SORPTION ENHANCED BIOGAS STEAM REFORMING USING NICKEL-BASED CATALYSTS

Mr. Janewit Phromprasit

A Thesis Submitted in Partial Fulfillment of the Requirements

for the Degree of Master of Engineering Program in Chemical Engineering

Department of Chemical Engineering

Faculty of Engineering

Chulalongkorn University

Academic Year 2011

Thesis Title   HYDROGEN PRODUCTION VIA SORPTION ENHANCED BIOGAS STEAM REFORMING USING NICKEL-BASED CATALYSTS

By   Mr. Janewit Phromprasit

Field of Study   Chemical Engineering

Thesis Advisor   Professor Suttichai Assabumrungrat, Ph.D.

_____

Accepted by the Faculty of Engineering, Chulalongkorn University in Partial Fulfillment of the Requirements for the Master's Degree

………………………….…..Dean of Faculty of Engineering

(Associate Professor Boonsom Lerdhirunwong, Dr.Ing.)

THESIS COMMITTEE

……………………………….Chairman

(Associate Professor Muenduen Phisalaphong, Ph.D.)

……………………………….Thesis Advisor

(Professor Suttichai Assabumrungrat, Ph.D.)

……………………………….Examiner

(Associate Professor Artiwan Shotipruk, Ph.D.)

……………………………….External Examiner

(Peangpit Wongmaneenil, D.Eng.)

เจนวิทย์ พรหมประสิทธิ์: การผลิตไฮโดรเจน ผ่านปฏิกิริยารีฟอร์มมิงแก๊ซชีวภาพด้วยไอน้ำที่ส่งเสริมด้วยการดูดซับโดยใช้นิกเกิลเป็นตัวเร่งปฏิกิริยา. (HYDROGEN PRODUCTION VIA SORPTION ENHANCED BIOGAS STEAM REFORMING USING NICKEL-BASED CATALYSTS) อ.ที่ปรึกษาวิทยานิพนธ์หลัก: ศ.ดร.สุทธิชัย อัสสะบำรุงรัตน์, 76 หน้า.

การผลิตไฮโดรเจน ผ่านปฏิกิริยารีฟอร์มมิงแก๊ซชีวภาพด้วยไอน้ำที่ส่งเสริมด้วยการดูดซับ คือกระบวนการที่รวมกระบวนการดูดซับแก๊สคาร์บอนไดออกไซด์กับกระบวนการผลิตแก๊สไฮโดรเจนเข้าด้วยกัน แคลเซียมออกไซด์ถูกเลือกมาเป็นตัวดูดซับเพราะว่ามีความจุการดูดซับสูงสุด (ร้อยละ 78.6) เมื่อเปรียบเทียบกับ Li_2ZrO_3, $K-Li_2ZrO_3$, Na_2ZrO_3 และ Li_4SiO_4 การทดลองการดูดซับแก๊สคาร์บอนไดออกไซด์โดยใช้แคลเซียมออกไซด์ถูกดำเนินการที่อุณหภูมิที่แตกต่างกัน (450, 500, 550 และ 600 องศาเซลเซียส) ผลการดูดซับแก๊สคาร์บอนไดออกไซด์แสดงค่าความจุการดูดซับที่มากที่สุดที่ 600 องศาเซลเซียส (0.2849 กรัมของคาร์บอนไดออกไซด์ต่อกรัมของแคลเซียมออกไซด์) นอกจากนี้ ผลของไอน้ำในสายป้อนของกระบวนการดูดซับแก๊สคาร์บอนไดออกไซด์จึงถูกพิจารณา ผลการทดลองพบว่าการดูดซับแก๊สคาร์บอนไดออกไซด์ที่มีไอน้ำในสายป้อน (0.6724 กรัมของคาร์บอนไดออกไซด์ต่อกรัมของแคลเซียมออกไซด์) มีค่ามากกว่าไม่มีไอน้ำในสายป้อน เพราะไอน้ำสามารถเพิ่มความจุในการดูดซับโดยการเพิ่มขึ้นของรูพรุนของแคลเซียมออกไซด์ สี่แบบของการจัดเรียงเบดถูกดำเนินการ โดยปฏิกิริยารีฟอร์มมิงแก๊สชีวภาพด้วยไอน้ำที่ส่งเสริมด้วยการดูดซับ ที่ไอน้ำต่อคาร์บอนเท่ากับ 3 มีเทนต่อคาร์บอนไดออกไซด์เท่ากับ 1.5 อุณหภูมิของปฏิกิริยาเท่ากับ 600 องศาเซลเซียส และที่ความดันบรรยากาศ ผลการทดลองพบว่า การจัดเรียงเบดแบบที่ 2 (นิกเกิล ร้อยละ 12.5 โดยน้ำหนัก บนอลูมิน่าผสมกับแคลเซียมออกไซด์) แสดงค่าการแปรผันของมีเทนเพิ่มขึ้นมากที่สุด (ร้อยละ 93 ด้วยผลของการดูดซับแก๊สคาร์บอนไดออกไซด์และร้อยละ 80 ไม่มีผลของการดูดซับแก๊สคาร์บอนไดออกไซด์) และความบริสุทธิ์ของผลิตภัณฑ์แก๊สไฮโดรเจน (ร้อยละ 97.3 ด้วยผลของการดูดซับแก๊สคาร์บอนไดออกไซด์และร้อยละ 60 ไม่มีผลของการดูดซับแก๊สคาร์บอนไดออกไซด์) เป็นที่ชัดเจนว่าเมื่ออุณหภูมิของปฏิกิริยาต่ำเท่ากับ 500 องศาเซลเซียส ถูกทำการทดลอง ค่าการแปรผันของมีเทนจะถูกทำให้มีค่ามากขึ้น (ร้อยละ 91.2 ด้วยผลของการดูดซับแก๊สคาร์บอนไดออกไซด์และร้อยละ 27 ไม่มีผลของการดูดซับแก๊สคาร์บอนไดออกไซด์) นอกจากนี้ เมื่อตัวเร่งปฏิกิริยาถูกเติมบนตัวดูดซับที่เป็นตัวรองรับ (นิกเกิล ร้อยละ 12.5 โดยน้ำหนัก บนแคลเซียมออกไซด์ และ นิกเกิล ร้อยละ 5.4 โดยน้ำหนัก บนแคลเซียมออกไซด์) จะพบการเสื่อมสภาพเกิดขึ้น

ภาควิชา ....วิศวกรรมเคมี........... ลายมือชื่อนิสิต ....

สาขาวิชา ....วิศวกรรมเคมี........... ลายมือชื่อ อ.ที่ปรึกษาวิทยานิพนธ์หลัก ....

ปีการศึกษา ....2554..................

5370413721: MAJOR CHEMICAL ENGINEERING

KEYWORDS: SORPTION ENHANCED/ BIOGAS STEAM REFORMING/ CALCIUM OXIDE/ HYDROGEN PRODUCTION

JANEWIT PHROMPRASIT: HYDROGEN PRODUCTION VIA SORPTION ENHANCED BIOGAS STEAM REFORMING USING NICKEL-BASED CATALYSTS. THESIS ADVISOR: PROF. SUTTICHAI ASSABUMRUNGRAT, Ph.D., 76 pp.

Hydrogen production via sorption enhanced biogas steam reforming is a process that combines CO_2 adsorption and hydrogen production in one unit operation. CaO is selected as an adsorbent because it has the highest stoichiometric adsorption capacity (78.6%) when compared with Li_2ZrO_3, $K-Li_2ZrO_3$, Na_2ZrO_3 and Li_4SiO_4. CO_2 adsorption tests of CaO were carried out at different temperatures (450, 500, 550 and 600 °C). The CO_2 sorption results showed the highest adsorption capacity at 600 °C (0.2849 g_{CO2}/g_{CaO}). In addition, the effect of steam in the feed of the CO_2 sorption process was considered. The results indicated that CO_2 sorption with the presence of steam (0.6724 g_{CO2}/g_{CaO}) was higher than that without steam effect because steam can increase adsorption capacity by increasing CaO porosity. Four types of bed arrangement for sorption enhanced biogas steam reforming at S/C of 3, CH_4/CO_2 of 1.5, reaction temperature of 600 °C and atmospheric pressure were performed. The results exhibited that bed arrangement type II (12.5 wt.% Ni/Al_2O_3 mixed with CaO) offered the highest improvement of CH_4 conversion (93% with CO_2 sorption effect and 80% without CO_2 sorption effect) and of purity of hydrogen product (97.3% with CO_2 sorption effect and 60% without CO_2 sorption effect). It was clear that when a lower reaction temperature of 500 °C was tested, the higher improvement of CH_4 conversion was increased (91.2% with CO_2 sorption effect and 27% without CO_2 sorption effect). Furthermore, when the catalyst was loaded on adsorbent as support (12.5 wt.% Ni/CaO and 5.4 wt.% Ni/CaO), the deactivation was observed.

Department: …..Chemical Engineering…... Student's Signature ……...……………..
Field of Study: Chemical Engineering…... Advisor's Signature …………………….
Academic Year: ………2011……………….

ACKNOWLEDGEMENTS

Firstly, the author would like to thank his advisor, Professor Suttichai Assabumrungrat, Ph.D., for his advices and suggests to successful in him life, study and research. Their suggestions give him to be good person in society, positive thinking, strength and happiness when him do this thesis.

Secondly, the author would like to grateful to Associate Professor Muenduen Phisalaphong, Ph.D., as the chairman, Associate Professor Artiwan Shotipruk, Ph.D., and Peangpit Wongmaneenil, D.Eng., as the examiner and Jonathan Powell, Ph.D. for their useful comments.

Furthermore, the author would like to thank his friends in Center of Excellence of Catalysis and Catalytic Reaction Engineering, Department of Chemical Engineering, Faculty of Engineering, Chulalongkorn University to help, suggest, teach him to successful in this project.

Finally, the author would like to thank his parent including dad, mom and older sister. They always support the author everything that they can do. The author cannot finish his thesis without their encouragements. The author would like to say he love his parent.

CONTENTS

LIST OF TABLES

LIST OF FIGURES

FIGURE   **PAGE**

FIGURE   **PAGE**

FIGURE **PAGE**

CHAPTER I

INTRODUCTION

1.1 Rationale

The world energy demand is increasing significantly due to the industrial development of countries such as Brazil, China and India (Westermann *et al.*, 2007) and an increasing world population. Most of the world energy is sourced from fossil fuels such as petroleum, natural gas and coal. The use of fossil fuels as an energy source has several environment problems attributed to gases emitted during the combustion process such as the 'green house' effect and acid rain due to the emission of air pollutants like CO_2, CO, H_2S and so on. It is well established that a solution to these global problems would be to replace the use of fossil fuels with renewable energy sources (Kalinci *et al.*, 2009).

Renewable energy includes energy sourced from natural resources such as sunlight, hydro, wind, biomass, bio-fuel and hydrogen. Solar energy is energy sourced from solar radiation. The solar cell is used for changing solar radiation to electricity but the efficiency of solar cell only around 24.7 % for monocrytalline silicon at solar intensity of 1,000 W/m^2 and cell temperature of 25 °C (Cited in Tiwari *et al.*, 2011). Hydro energy is energy obtained from large scale dams that use high water flow for producing electricity. Wind energy is energy generated from airflows using wind turbines to generate electricity. These can only be used in locations where winds are strong and constant, such as offshore and high altitude sites. Biomass energy is energy from plant material such as wood, waste, agricultural products and so on. Moreover, the interesting renewable energy is hydrogen energy carrier particularly useful as an energy source in fuel cell and batteries.

Hydrogen gas (H_2) is a clean and sustainable fuel considered to be an alternate to resolve the energy problems in the future (Liu *et al.*, 2009). Hydrogen is a chemical element found in organic compounds (i.e. CH_4 which has the highest hydrogen to carbon ratio). Furthermore, the energy density of H_2 is approximately 142 MJ/kg,

being more heating energy than coal about 4 times and more than natural gas about 3 times. Combustion of hydrogen produces clean products that generate only water and energy shown in equation (1.1) while combustion of hydrocarbons produces pollutants including CO_2 as shown in equation (1.2).

Hydrogen can be produced by several processes such as electrolysis which is a process to separate water to hydrogen and oxygen as shown in equation (1.3) but it must operate at high pressure condition, meaning that they must use high energy on pump and compressor (Laoun., 2007). Solar biological process uses the cyanobacteria and the sunlight to produce O_2, with H_2 gas as a side product, but is currently limited by a poor H_2 yield (Carrieri *et al.*, 2008). Photocatalysis is a process that uses ultraviolet or visible light and a photocatalyst to produce hydrogen. Photocatalysts are such as TiO_2 (Moon *et al.*, 2000) and B for ultraviolet light, and Cr, Fe, V and Pt over TiO_2 for visible light (Moon *et al.*, (2000); Dholam *et al.*, (2009); Sreethawong *et al.*, (2009); Dholam *et al.*, (2011)) but it requires a large process because it has small H_2 production rate for example Fe-doped TiO_2 and Cr-doped TiO_2 have H_2 production rate of 15.5 μmole/h and 5.3 μmole/h, respectively (Dholam *et al.*, 2009). Steam reforming is a process that is famous in hydrogen production industry. Water (steam) can reform large hydrocarbons to small molecular hydrocarbons or hydrogen and carbon dioxide (CO_2) via catalyst.

$$2H_2 + O_2 \leftrightarrow 2H_2O + \text{Energy} \qquad \dots (1.1)$$

$$C_xH_y + (x+y/2)O_2 \leftrightarrow xCO_2 + y/2H_2O \qquad \dots (1.2)$$

$$2H_2O \text{ (liq)} + \text{Electrical energy} \leftrightarrow 2H_2 + O_2 \qquad \dots (1.3)$$
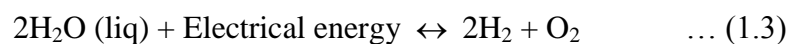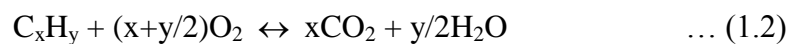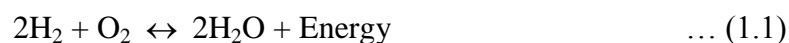
Steam reforming can use several reactants such as methane, methanol, and ethanol for hydrogen production. A number of researches have been focused on various steam reforming reactions, for example, methane steam reforming (Pistonesi *et al.*, (2007); Lertwittayanon *et al.*, (2010); Maluf *et al.*, (2009); Essaki *et al.*, (2008)), methanol steam reforming (Peppley *et al.*, (1999); Hong *et al.*, (2008); Huang *et al.*, (2010); Basile *et al.*, (2008)) and ethanol steam reforming (Casanovas *et*

al., (2009); Carrero *et al.*, (2010); Youn *et al.*, (2010)). The main reactions are shown in equations (1.4) – (1.6), respectively.

$$CH_4 + H_2O \leftrightarrow CO + 3H_2 \qquad \qquad \dots (1.4)$$

$$CH_3OH + H_2O \leftrightarrow CO_2 + 3H_2 \qquad \qquad \dots (1.5)$$

$$C_2H_5OH + 3H_2O \leftrightarrow 2CO_2 + 6H_2 \qquad \qquad \dots (1.6)$$
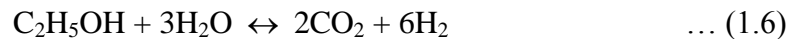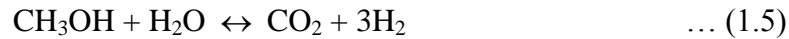
Moreover, dry methane reforming is one of the most common reactions to produce hydrogen (Frusteri *et al.*, (2001); Juan *et al.*, (2006)) a shown in equation (1.7).

$$CH_4 + CO_2 \leftrightarrow 2CO + 2H_2 \qquad \qquad \dots (1.7)$$
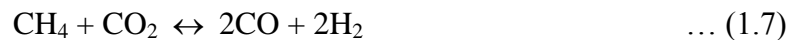
Nowadays, biogas is of particular interest. It is produced by anaerobic digestion or fermentation of biodegradable materials such as green waste, manure and so on. Biogas has main compositions of methane (CH_4) and carbon dioxide (CO_2) which can be combined with steam reforming to produce hydrogen as shown in equation (1.8) (Avraam *et al.*, 2010). The advantage of biogas steam reforming is that it involves two reactions in one process for hydrogen production, dry methane reforming and steam methane reforming. Water gas shift (WGS) reaction shown in equation (1.9) also takes place to further increase H_2 production. The disadvantages of biogas steam reforming are impurities in product stream (CO_2 and CO) and coke formation on catalysts.

$$2CH_4 + CO_2 + H_2O \leftrightarrow 5H_2 + 3CO \qquad \qquad \dots (1.8)$$

$$CO + H_2O \leftrightarrow H_2 + CO_2 \qquad \qquad \dots (1.9)$$
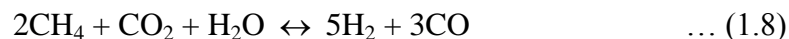
Sorption enhanced reaction is a process that simultaneously removes a product by adsorption during a reaction taking place, and thus shifts the forward reaction to more completion. For sorption enhanced steam reforming reaction, CO_2 can be selectively separated from the reaction mixture using various available sorbents such as hydrotalcite (Reijers *et al*., 2006; Oliveira *et al*., 2008), dolomite (Hildenbrand *et al.,* 2006), calcium oxide (Martavaltzi *et al*., 2010) and lithium zirconate (Ochoa-

Fernández *et al*., 2007) to promote hydrogen production and purification. Among various adsorbents, calcium oxide shows the highest stoichiometric capacity (78.6%) when compared with Li_2ZrO_3 (28.8%), Na_2ZrO_3 (23.4%) and Li_4SiO_4 (36.6%) (Ochoa-Fernández *et al*., 2007). The improvement of hydrogen production from methane steam reforming in a single-step process was studied by Balasubramanian *et al*., (1999). CaO was used as a CO_2 acceptor, the results showed that 95% hydrogen purity was achieved at a temperature of 650 °C and pressure of 15 atm while only 65% hydrogen was obtained when without using CaO. In addition, the Ni/CaO multifunctional catalyst for hydrogen production via sorption enhanced steam methane reforming was investigated by Chanburanasiri *et al*., (2011). They found that 12.5 wt.% Ni/Al_2O_3+CaO exhibited the highest CH_4 conversion (89%) when compared with 12.5 wt.% Ni/CaO (86%) and 12.5 wt.% Ni/Al_2O_3 (84%, without adsorption effect). Moreover, the 12.5 wt.% Ni/Al_2O_3+CaO showed the highest purity of H_2 (83%) when compared with 12.5 wt.% Ni/CaO (82%), 12.5 wt.% Ni/MG30-K (75%) and 12.5 wt.% Ni/Al_2O_3 (72%). The same concept of hydrogen production has been applied to steam reforming of other feedstocks such as propane (Wang *et al*., 2011), glycerol (Dou *et al*., 2009), ethanol (Essaki *et al*., 2008), methanol and n-butanol (Silva *et al*., 2011). However, the work on steam reforming of biogas containing high content of CO_2 in feed has not been well investigated. Therefore, this study will focus on the sorption-enhanced biogas steam reforming. Particular interest is on selection of catalyst-adsorbent bed arrangement to handle high content of CO_2 in the reaction system.

1.2 Objective

To develop a suitable bed arrangement of catalyst and adsorbent for hydrogen production via sorption enhanced steam reformation of biogas and to determine effects of operating parameters on the reaction performance.

1.3 Scope of work

- Three catalyst beds including 12.5 wt.% Ni/CaO, 12.5 wt.% $Ni/\gamma-Al_2O_3$ and 12.5 wt.% $Ni/\gamma-Al_2O_3$+CaO are considered. CaO is selected as an adsorbent

for adsorption of CO_2. The catalysts are prepared via conventional incipient wetness impregnation method.

- The catalysts are characterized to determine their physical properties. The techniques include X-ray diffraction (XRD) and N_2-Adsorption desorption.

- The reaction tests of sorption enhanced biogas steam reforming for hydrogen production are carried out at various operating conditions, for example, temperatures of 450-600 °C.

- Reaction performance in terms of hydrogen concentration and methane conversion from different catalyst bed arrangement is compared.

1.4 Research plan

- Review the hydrogen production from methane steam reforming, dry methane reforming, biogas steam reforming and sorption enhanced process.

- Prepare catalysts via conventional incipient wetness impregnation method.

- Characterize the catalysts using X-ray diffraction (XRD) and N_2-Adsorption desorption.

- Set up the experimental equipments.

- Investigate the performance of the reaction system including catalyst and adsorbent for biogas steam reformation in terms of methane conversion and gases composition.

- Conclude the results.

- Write the report.

CHAPTER II

BACKGROUND
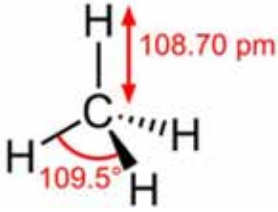
This chapter presents background information on biogas, hydrogen production via several processes such as steam methane reformation, dry methane reformation, biogas steam reforming, and fixed bed adsorption.
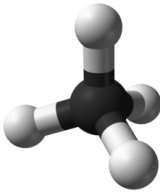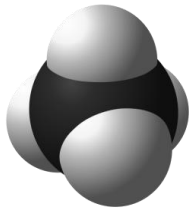
2.1 Definition

2.1.1 Methane (CH_4)

Methane is a smallest hydrocarbon compound, an odorless, a colorless and, a flammable gas. It has the highest carbon to hydrogen ratio of all hydrocarbons, with a value of 1:4. Some properties of methane are shown in Table 2.1. Normally, odorous organic sulfur compounds such as tertiary-butyl mercaptan ((CH_3)$_3$CSH) and dimethyl sulfide (CH_3–S–CH_3) are added to commercial natural gas for the purpose of making them detectable (http://scifun.chem.wisc.edu).

Table 2.1 Structure and properties of methane molecule.
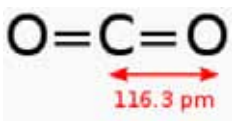
Molecular formula	CH_4
Structure	Structure and dimensions

	Ball and stick model Space filling model
Molar mass	16.04 g mol^{-1}
Appearance	Colorless gas
Density	0.717 kg/m^3 (gas, 0 °C) 416 kg/m^3 (liquid)
Melting point	−182.5 °C, 90.7 K, −296.5 °F
Boiling point	−161.6 °C, 111.6 K, −258.9 °F
Solubility in water	35 mg/L (17 °C)
Heating value	1000 BTU/cu ft

2.1.2 Carbon dioxide (CO_2)

Carbon dioxide is a chemical component that is composed of two oxygen atoms bonded to a single atom, and also colorless and odorless in its pure form. Commercially, carbon dioxide is used as a refrigerant and in fire extinguishers. Mostly, commercial carbon dioxide is a by-product of other processes such as ethanol production via fermentation and the breathing of humans. Some properties of carbon dioxide are shown in Table 2.2

Table 2.2 Structure and properties of carbon dioxide molecule.

Molecular formula	CO_2
Structure	Structure and dimensions 116.3 pm Ball and stick model Space filling model
Molar mass	44.01 g mol^{-1}
Exact mass	43.989829244 g mol^{-1}
Appearance	Colorless gas
Odor	Odorless
Density	1.562 g/mL (solid at 1 atm and −78.5 °C) 0.770 g/mL (liquid at 56 atm and 20 °C) 1.977 g/L (gas at 1 atm and 0 °C)
Melting point	-78 °C, 194.7 K, -109 °F
Boiling point	-57 °C, 216.6 K, -70 °F (at 5.185 bar)
Solubility in water	1.45 g/L at 25 °C, 100 kPa
Acidity (pK_a)	6.35, 10.33
Refractive index (n_D)	1.1120
Viscosity	0.07 cP at −78 °C
Dipole moment	zero

2.1.3 Biogas

Biogas is a gas produced by the anaerobic digestion or fermentation of a biodegradable substrate such as biomass, where the proteins, carbohydrates and lipids contained within the biomass are broken down into small molecules such as fatty acid and biogas by biological processes. The composition of biogas is typically 55-70 % of methane, 27-44 % of carbon dioxide and 2-3 % of nitrogen, hydrogen and hydrogen sulfide (Kolbitsch *et al*., 2008).

Biogas is commonly produced by one of several processes which include the fixed dome floating drum and channel balloon processes. They are easy to build, comfortable, durable and low maintenance. Figures 2.1 and 2.2 show fixed dome type biogas plant and floating gas-holder type biogas plant, respectively.
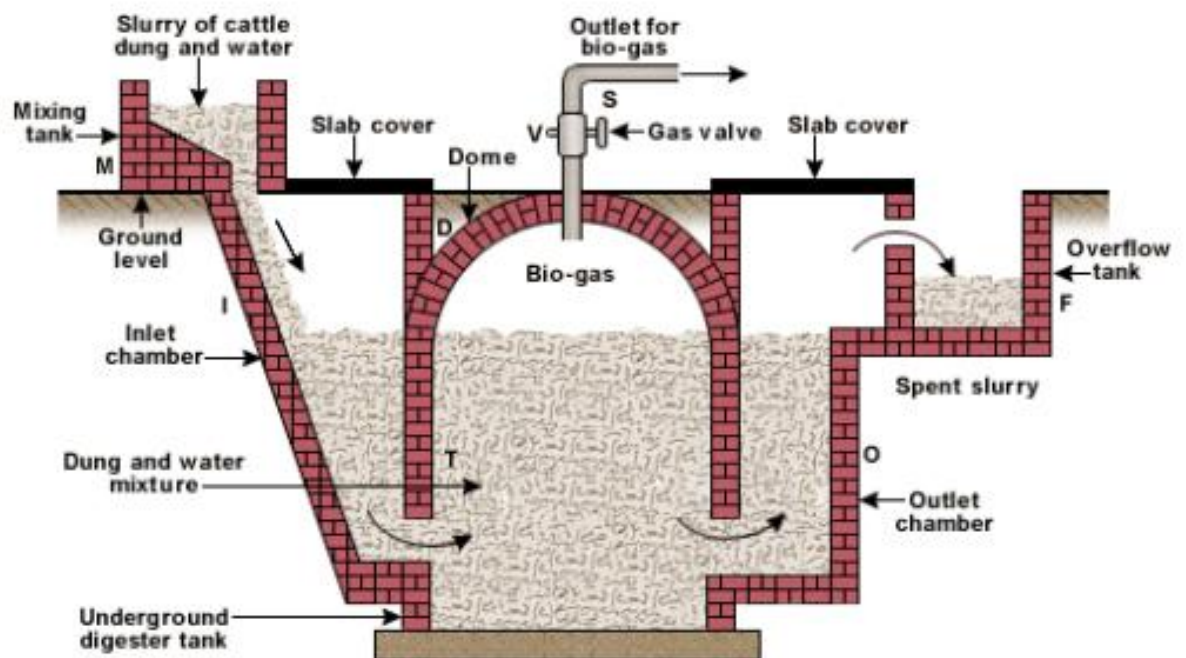
Figure 2.1 Fixed-dome type bio-gas plant.
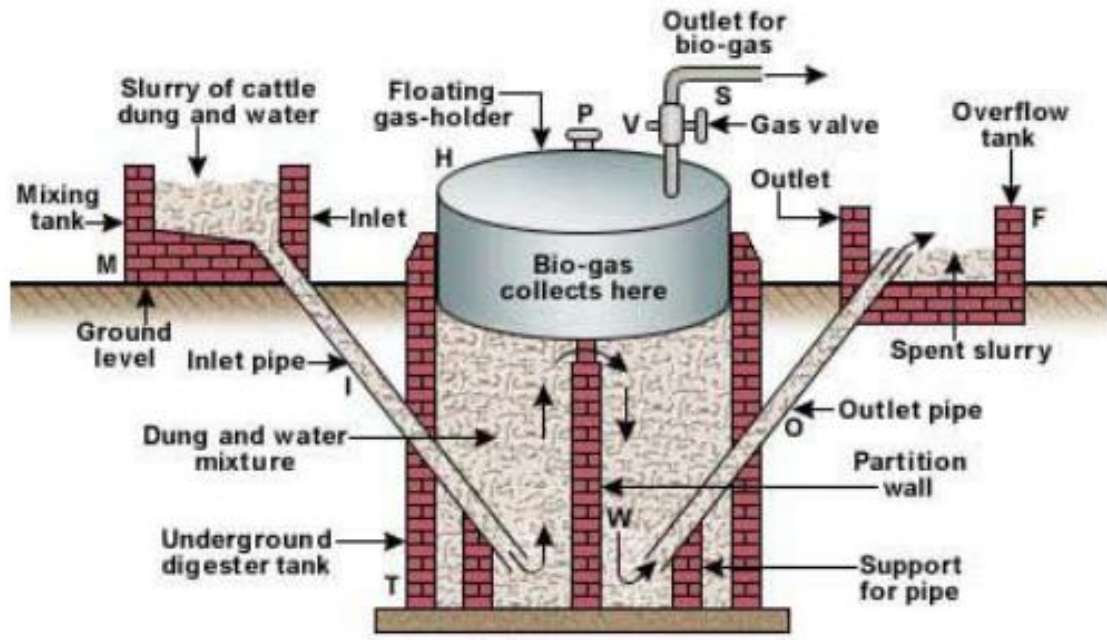
Figure 2.2 Floating gas-holder type bio-gas plant.

2.2 Reforming process

2.2.1 Steam methane reforming

Steam methane reforming (SMR) is a leading process for hydrogen production in industry. Steam methane reforming includes the steam reforming reaction and water gas shift reaction (WGSR) as shown in equations (2.1) and (2.2), respectively. The steam reforming reaction is highly endothermic but the side reaction is water gas shift reaction that is an exothermic reaction (Lertwittayanon *et al.*, 2010). ΔH_R indicates the standard of enthalpy change at a pressure of 1 atm and a temperature of 25 °C that shows in the right hand side of the reaction.

$$CH_4 + H_2O \leftrightarrow 3H_2 + CO \qquad \Delta H^0_{298} = +206 \text{ kJ/mol} \qquad \ldots (2.1)$$

$$CO + H_2O \leftrightarrow H_2 + CO_2 \qquad \Delta H^0_{298} = -41.1 \text{ kJ/mol} \qquad \ldots (2.2)$$

Ni-Al$_2$O$_3$ catalyst is commonly used as catalyst for steam methane reforming because it has high activity and low cost (Lertwittayanon *et al.*, 2010; Essaki *et al.*,

2008). However, it is prone to deactivation by carbonaceous species such as coke and carbon from several reactions such as methane cracking, boudouard reaction, and CO reduction to carbon as shown in equations (2.3) – (2.5), respectively.

$$CH_4 \quad \leftrightarrow \quad C + 2H_2 \qquad \Delta H^0_{298} = +75 \text{ kJ/mol} \qquad \ldots (2.3)$$

$$2CO \quad \leftrightarrow \quad C + CO_2 \qquad \Delta H^0_{298} = -172.5 \text{ kJ/mol} \qquad \ldots (2.4)$$

$$CO + H_2 \quad \leftrightarrow \quad C + H_2O \qquad \Delta H^0_{298} = -131.3 \text{ kJ/mol} \qquad \ldots (2.5)$$

$$CH_4 + 2H_2O \quad \leftrightarrow \quad 2CO_2 + 4H_2 \quad \Delta H^0_{298} = +165 \text{ kJ/mol} \qquad \ldots (2.6)$$

Figure 2.3 shows the schematic flow sheet of a conventional steam methane reforming process, the first step is indicated by equations (2.1) and (2.6). Methane reacts with steam, which are fed into the furnace producing hydrogen and carbon dioxide. The reaction is carried out at a temperature within the range of 800-1000 °C and a pressure of 14-20 atm over nickel based catalysts. The second step is illustrated by equation (2.2). The water gas shift reaction (WGS) is carried out at temperatures within the range of 300-400 °C. The last step presents CO_2 removal by amine scrubbing to purify H_2 (up to 99%) (Barelli *et al.,* 2008).
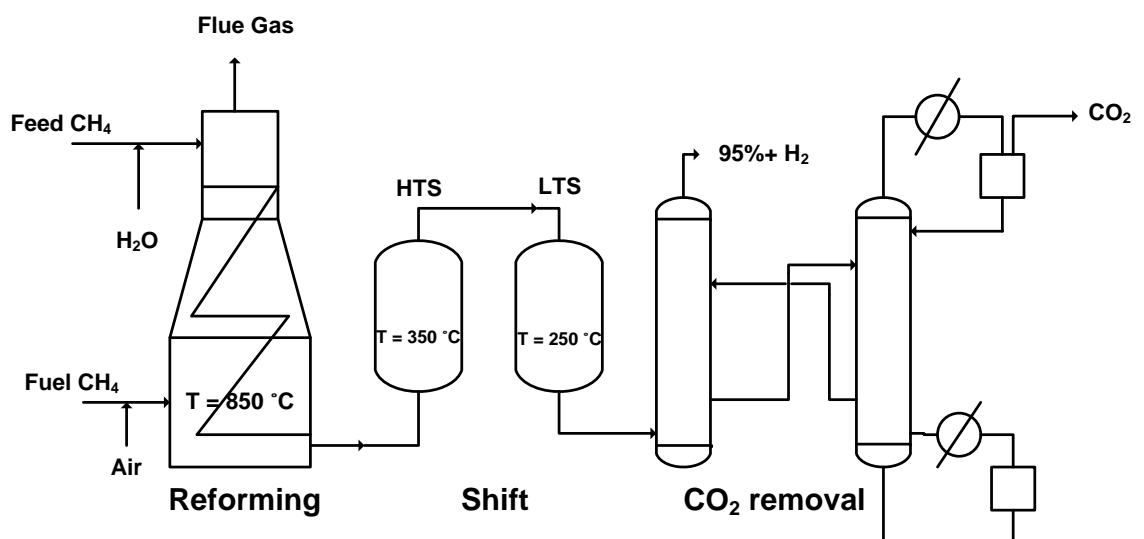
Figure 2.3 Flowsheet for a conventional SMR process. (Barelli *et al.,* 2008)

2.2.2 Dry methane reforming

Dry methane reforming is also a process for hydrogen production. The main reactants are methane and carbon dioxide, and the main products are hydrogen and carbon monoxide as shown in equation (2.7) (Muradov *et al*., 2008). Not only hydrogen and carbon monoxide but also carbon can be produced, resulting in carbon or coke deposition over the catalyst and support as illustrated in equation (2.3) and (2.4) (San-José-Alonso *et al*., 2009) which is the main cause of catalyst deactivation.

$$CH_4 + CO_2 \leftrightarrow CO + H_2 \qquad \Delta H^0_{298} = +247 \text{ kJ/mol} \qquad \ldots (2.7)$$

Definition of parameters such as conversion and yield for CO_2 reforming with methane are calculated as shown in the following equations (2.8) – (2.12) (Djaidja *et al*., 2006).

$$CH_4 \text{ conversion } (\%) = \frac{moles \ of \ CH_4 \ converted}{moles \ of \ CH_4 \ in \ feed} \times (100 \ \%) \qquad \ldots (2.8)$$

$$CO_2 \text{ conversion } (\%) = \frac{moles \ of \ CO_2 \ converted}{moles \ of \ CO_2 \ feed} \times (100 \ \%) \qquad \ldots (2.9)$$

$$Yield \ of \ H_2 (\%) = \frac{moles \ of \ H_2 \ produced}{2 \ moles \ of \ CH_4 \ in \ feed} \times (100\%) \qquad \ldots (2.10)$$

$$Yield \ of \ CO (\%) = \frac{moles \ of \ CO \ produced}{moles \ of \ CH_4 \ in \ feed + moles \ of \ CO_2 \ in \ feed} \times (100\%) \qquad \ldots (2.11)$$

$$\frac{H_2}{CO} = \frac{moles \ of \ H_2 \ produced}{moles \ of \ CO \ produced} \qquad \ldots (2.12)$$

2.2.3 Biogas steam reforming

Biogas steam reforming is a process that uses methane, carbon dioxide, and steam as reactants. The product is syngas (H_2 + CO). The reaction mechanism of biogas steam reforming consists of four reactions including methane steam reforming shown in equations (2.1) and (2.6), water gas shift shown in equation (2.2), and dry methane reforming shown in equation (2.7).
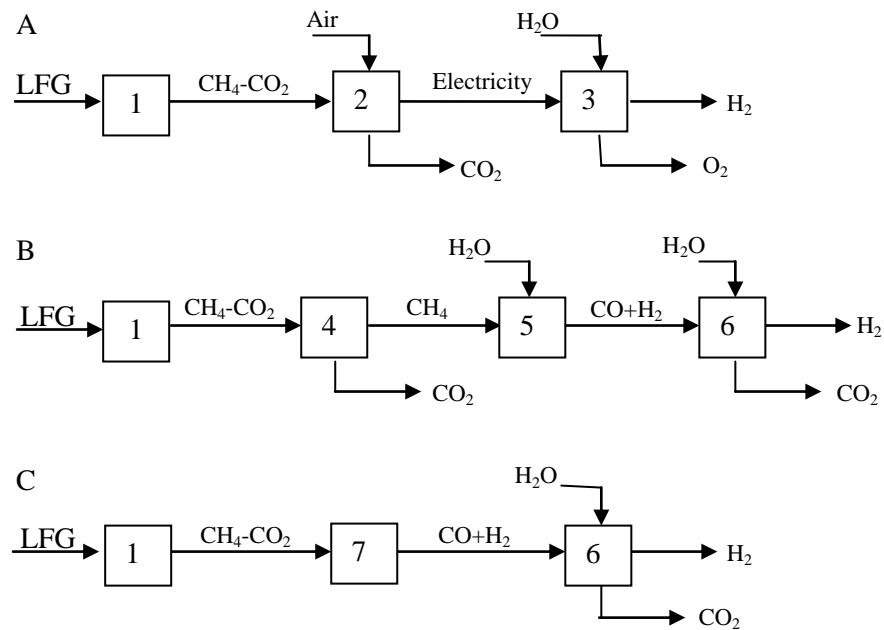
Figure 2.4 Three pathways to produce hydrogen from landfill gas (LFG): (A) LFG combustor coupled with a turbine and an electrolyzer, (B) preliminary separation of methane coupled with steam methane reforming unit, (C) direct reforming of LFG. (Muradov *et al*., 2008)

In principle, three pathways to produce hydrogen from landfill gas (LFG) are used for hydrogen production (Muradov *et al*., 2008) as shown in Figure 2.4. Figure 2.4 (A) represents a process where LFG is combusted in a turbine (2), the products are CO_2 and electricity which can be used as energy for splitting water as indicated in step (3), resulting in hydrogen and oxygen as products. Figure 2.4 (B) indicates that methane is separated from carbon dioxide (4) by conventional technologies such as amine scrubbing, selective adsorption and so on. Then syngas is produced via steam methane reforming process (5) and the concentration of hydrogen increases by water gas shift unit (6). Figure 2.4 (C) illustrates a directly reformed process (7) produces syngas without first separated methane after that hydrogen is increased via WGS unit (6).

Definitions of the parameters are described for biogas steam reforming such as steam to carbon ratio (equation (2.13)), space velocity (equation (2.14)), conversion (equation (2.15)), H_2 yield (equation (2.16)), and CO selectivity (equation (2.17)):

Steam/carbon molar ratio:

$$S/C = \frac{Y_{H_2O,in}}{Y_{CH_4,in}} \qquad \text{(mol/mol)} \qquad \ldots (2.13)$$

Space velocity (SV):

$$SV = \frac{V_{in}}{m_{cat}} \qquad \text{(m}^3 \text{ h}^{-1} \text{ kg}^{-1}) \qquad \ldots (2.14)$$

The conversions of substance x:

$$Conversion\ (x) = \frac{N_{x,BG} - N_{x,SG}}{N_{x,BG}} \times (100\%) \qquad \ldots (2.15)$$

H₂ yield:

$$H_2\ yield = \frac{N_{H_2,SG}}{N_{CH_4,BG}} \frac{1}{4} \qquad \ldots (2.16)$$

CO selectivity:

$$CO\ selectivity = \frac{Y_{CO,SG}}{Y_{CO,SG} + Y_{CO_2,SG}} \qquad \ldots (2.17)$$

2.2.4 Fixed bed adsorption

Adsorption in a fixed bed, the concentrations of fluid phase and solid phase change with time and position in the bed. The adsorption occurs at origin of adsorbents, then the equilibrium between fluid and solid adsorbents are achieved. The results are shown in Figure 2.5, called a *stoichimetric front*, the concentration of solute moves as a sharp concentration front through the bed. This is *ideal fixed bed adsorption*. Upstream of the front, the adsorbents are saturated with adsorbate and the concentration of solute in the fluid phase feed is called c_F. The loading of adsorbated on the adsorbent is the q_F in equilibrium with c_F. The length and weight of bed are LES and WES, respectively, where ES is equilibrium section. Downstream of the stoichiometric front and in the exit way, the concentration of the solute in stream is zero. The length and weight of this bed section are LUB and WUB, respectively, where UB is unused bed.
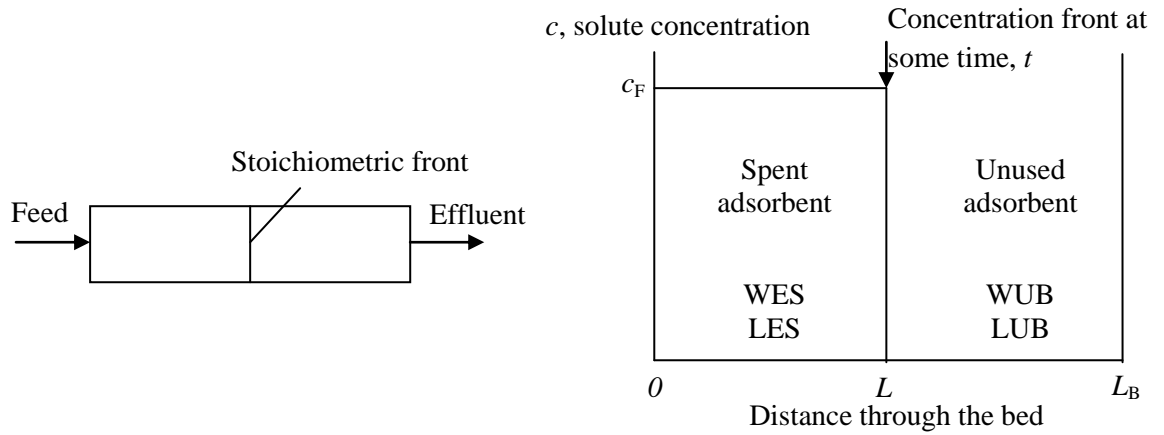
Figure 2.5 Stoichiometric (equilibrium) concentration front for ideal fixed bed adsorption.

After a period of time, the concentration of the solute rises to the inlet values, c_F, no further adsorption is possible, and the adsorption step is terminated. This point is referred to the *break point* (normally, c/c_F equal to 0.05 or 0.10) and stoichiometric wave front becomes the ideal *breakthrough curve*. For ideal fixed bed adsorption, material balance on the adsorbate before breakthrough occurs is: Solute in entering feed = adsorbate:

$$Q_F c_F t_{ideal} = q_F S L_{ideal}/L_B \qquad \dots (2.18)$$

Where Q_F is the volumetric flow rate of feed, c_F is the concentration of the solute in the fluid feed, t_{ideal} is time for an ideal front to reach $L_{ideal} < L_B$, q_F is the loading per unit mass of adsorbent that is in equilibrium with the feed concentration, S is the total mass of adsorbent in the bed, and L_B is the total bed length.

$$L_{ideal} = LES = \left(\frac{Q_F c_F t_{ideal}}{q_F S}\right) L_B \qquad \dots (2.19)$$

$$LUB = L_B - LES \qquad \dots (2.20)$$

$$WES = S\left(\frac{LES}{L_B}\right) \qquad \dots (2.21)$$

$$WUB = S - WES \qquad \dots (2.22)$$

In a real fixed bed adsorber, the assumptions of leading to equation are not valid. Typically, solute concentration profiles for the fluid are shown as a function of distance through the bed at increasing time t_1, t_2, and t_b from the start of flow through the bed that are shown in Figure 2.6 (a). At t_1, no part of the bed is saturated. At t_2, the bed is almost saturated for a distance L_s. At L_f, the bed is almost clean. Beyond L_f, little mass transfer occurs at t_2 and the adsorbent is still unused. The region between L_s and L_f is called the mass transfer zone, MTZ at t_2, L_f can be taken where $c/c_F = 0.05$, with L_s at $c/c_F = 0.95$. From t_2 to time t_b, the S shape move through the bed. At t_b, the leading point of MTZ reaches the end of the bed. This is breakthrough point. Rather than using $c/c_F = 0.05$, the breakthrough concentration can be taken as the minimum detectable or maximum allowable solute concentration in the effluent fluid.

Distance through bed,

(a)

(b)
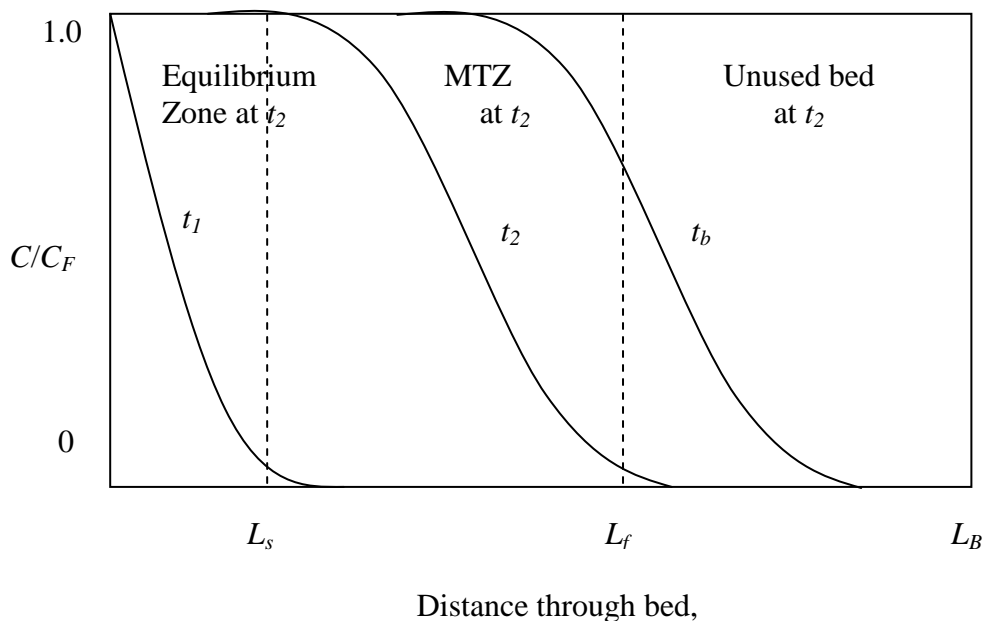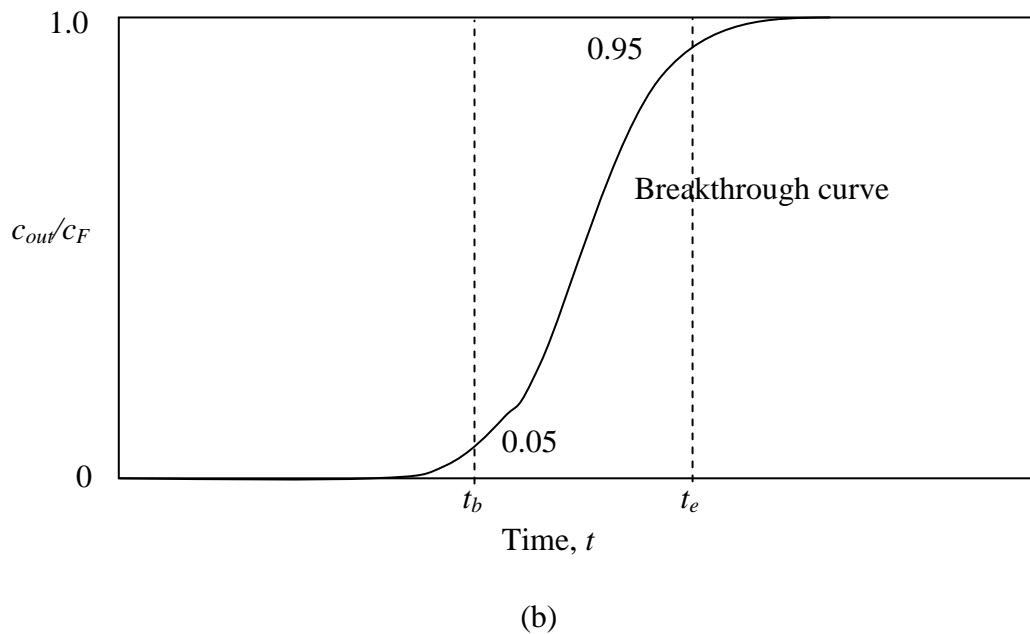
Figure 2.6 Solute wave fronts in a fixed bed adsorber with mass transfer effects.
(a) Concentration-distance profiles. (b) Breakthrough curve.

Typical plot of the ratio of the outlet to inlet solute concentration in the fluid as a function of time from the start of flow is shown in Figure 2.6 (b). The S-shaped curve is called breakthrough curve. Prior to t_b, the solute concentration is less than $c_{out}/c_F = 0.05$. At t_b is reached, the adsorption is discontinued, the regeneration is begun. At $t > t_b$, the outlet solute concentration is increased rapidly. The time to reach $c_{out}/c_F = 0.95$ is designated t_e.

CHAPTER III

LITERATURE REVIEWS

This chapter presents literature reviews of previous researches on steam reforming and more specifically steam methane reforming (SMR), dry methane reforming (DMR), biogas steam reforming, and sorption enhanced steam methane reforming process (SESMR).

3.1 Steam methane reforming

Steam methane reforming is a common process used in the production of hydrogen. The process provides many advantages including the production of methane with a high carbon to hydrogen ratio of 1:4 coupled with the many industrial processes having the advantage of having a water decomposition step. Furthermore, the presence of water can assist to reduce the amount of coke or carbon deposition on the catalyst surface, whilst it also increases the heat conductivity within the reactor. Therefore, many researchers had investigated steam methane reforming about activity, selectivity, and stability of catalysts.

Catalyst activity is commonly investigated research area, for which some the researchers are shown in Table 3.1. Research had been carried out on new catalysts, promoters and supports such as Ni to increase catalyst activities (Maluf *et al.*, 2009), ZrO_2 (Matsumura *et al*., (2004); Zhang *et al*., (2004)), perovskites (Urasaki *et al.*, 2005) and so on. Maluf *et al.*, (2009) reported on research regarding the use of Ni/Al_2O_3 catalysts with Mo promoter for methane steam reforming. The NiO/Al_2O_3 catalyst was synthesized via simultaneous precipitation method and promoted with Mo oxide approximately 0.05, 0.5, 1 and 2 wt.%. The operating conditions of feed were steam/methane of 4:1 and 2:1. The results showed that all composition of Mo promoter except 1.0 wt.% had high stability at steam/methane of 4:1 for nearly 30 hours. However, at feed steam/methane of 2:1 had only one composition of Mo promoter that was 0.05 wt.% Mo which was stable throughout $8 - 9$ hours of the experiment. Urasaki *et al.*, (2005) studied about catalytic activity of Ni over

perovskites compared with Ni over α-Al_2O_3 for methane steam reforming reaction. The perovskites as supports included $LaAlO_3$, $LaFeO_3$, $SrTiO_3$, $BaTiO_3$, and $La_{0.4}Ba_{0.6}Co_{0.2}Fe_{0.8}O_{3-\delta}$. The operating conditions were temperature of 800 °C, pressure of 0.1 MPa, and steam/methane of 2. The results exhibited that catalytic activity of Ni/$LaAlO_3$ and Ni/$SrTiO_3$ was highest activity with CH_4 conversion of 91.7 and 88.4%, respectively at 1 hour of reaction. Not only Al_2O_3 and perovskites as support but also ZrO_2 as a support indicated high activity for steam methane reforming. For example, Matsumura *et al.*, (2004) studied different kind of supports including SiO_2, Al_2O_3, and ZrO_2 over 20wt.% nickel catalysts for hydrogen production at low temperature. The operating conditions were temperature of 500 °C, catalysts of 0.3 g, steam to carbon ratio of 2 and reduction temperature of 700 °C. The best support that exhibited the highest CH_4 conversion was ZrO_2 with CH_4 conversion of 25.5 %. Furthermore, Zhai *et al.,* (2011) investigated about three Ni-based catalysts were Ni/ZrO_2/Al_2O_3, Ni/La-Ca/Al_2O_3, and $Ni_{0.5}Mg_{2.5}AlO_9$ for hydrogen production via steam methane reforming at high space velocity. The catalysts were prepared by impregnating method, and Ni loading was about 20 wt.%. The operating conditions were steam to carbon ratio of 3, gas hourly space velocity was varied from 6.0 x 10^4 h^{-1} to 1.2 x 10^6 h^{-1}, and the catalysts were reduced with hydrogen at 900 °C for 30 min. The experimental results indicated that $Ni_{0.5}Mg_{2.5}AlO_9$ had the high reaction performance (i.e. activity and stability).

The stabilities of catalysts were important for industrial operations to produce the hydrogen from steam methane reforming. The catalyst deactivation was a problem for stabilities of catalysts. The main cause of catalyst deactivation for steam methane reforming was coke and carbon formation that are shown in equation (2.3) − (2.5). Many researchers had investigated catalysts to solve this problem. For example, Urasaki *et al.*, (2005) studied about coking resistance of Ni/perovskites in steam reforming of methane. The operating conditions were steam/methane ratios of 1, temperature of 800 °C, and pressure of 0.1 MPa. The Ni over $LaAlO_3$ showed high CH_4 conversion stability, maintaining CH_4 conversion of 77 − 80% for 24 hours, while Ni over α-Al_2O_3 was deactivated via coke formation, and CH_4 conversion decreased from 83% at 2 hours to 75% at 24 hours. Inactive carbon species were

observed to form on Ni/α-Al$_2$O$_3$ but they were not observed on Ni/LaAlO$_3$ and LaAlO$_3$ supports that could prevent the formation of inactive carbon species. Moreover, many researchers modified supports like Al$_2$O$_3$ with CeO$_2$ and ZrO$_2$ (Pompeo *et al.*, (2009); Dong *et al.*, (2002); Roh *et al.*, (2002)). For example, Pompeo *et al.*, (2009) improved the stability of Ni/α-Al$_2$O$_3$ via CeO$_2$ and ZrO$_2$. The five compositions of catalyst were investigated including Ni/αAl$_2$O$_3$, Ni/5CeαAl$_2$O$_3$, Ni/4Ce1ZrαAl$_2$O$_3$, Ni/2.5Ce2.5ZrαAl$_2$O$_3$, Ni/1Ce4ZrαAl$_2$O$_3$, and Ni/5ZrαAl$_2$O$_3$. The operating conditions were temperature of 500-700 °C, GHSV of 3 x 10^5 cm^3/hg, pressure of 1 atm, N$_2$/CH$_4$/H$_2$O of 10/2/2,and reduction temperature of 700 °C for 1 hour in H$_2$ (30 cm^3/min). The optimal temperature was 700 °C, CH$_4$ conversions of Ni/4Ce1ZrαAl$_2$O$_3$, Ni/1Ce4ZrαAl$_2$O$_3$, Ni/2.5Ce2.5ZrαAl$_2$O$_3$, Ni/5ZrαAl$_2$O$_3$, Ni/5CeαAl$_2$O$_3$, and Ni/αAl$_2$O$_3$ were 66, 57, 55, 50, 46.5 and 45 %, respectively. In 2002, Dong *et al.*, (2002) varied the nickel content over Ce-ZrO$_2$. The operating conditions were temperature of 750 °C, Steam to carbon ratios of 3, CH$_4$ flow rate of 30 ml/min, and N$_2$ flow rate of 30 ml/min. Nickel loading of 3, 10, 15, 20 and 30 were studied. 15 wt.% Ni/Ce-ZrO$_2$ exhibited highest CH$_4$ conversion that was 97.0 %. Furthermore, Zhang et al., (2004) compared between nanoparticles and conventional of ZrO$_2$ with Al$_2$O$_3$ commercial which were loaded with Ni catalyst. They were investigated about stability and activity of catalyst. The operating conditions were atmospheric pressure, temperature of 800 °C, and GHSV$_{CH_4}$ of 12,000 ml/(h g$_{cat}$). All catalysts exhibited high stability and activity for 240 h. The CH$_4$ conversions were 87-88 %, 81-84 % and 76-83 % for Ni/ZrO$_2$-AN, Ni/Al$_2$O$_3$ and Ni/ZrO$_2$-CP, respectively.

Table 3.1 Summary of previous works with different catalysts, supports and conditions for steam methane reforming reaction.

Catalyst	Amount (g)	Condition		CH$_4$ Conversion (%)	Ref.
		Temp. (°C)	S/C		
20wt.% Ni/SiO$_2$[a]	N/A	500	2.0	14.8	Matsumu ra *et al.*, (2004)
20 wt% Ni/Al$_2$O$_3$[b]	N/A	500	2.0	17.4	
5 wt.% Ni/ZrO$_2$[b]	N/A	500	2.0	21.3	

20 wt.% Ni/ZrO$_2$[b]	N/A	500	2.0	25.5	
12.1 wt.% Ni/ZrO$_2$-AN[c]	N/A	800	1.0	87-88	Zhang *et*
12.9 wt.% Ni/ZrO$_2$-CP[d]	N/A	800	1.0	81-84	*al.*,
13.0 wt.% Ni/Al$_2$O$_3$-C[e]	N/A	800	1.0	76-83	(2004)
2 wt.% Ni/αAl$_2$O$_3$	N/A	700	1.0	45	Pompeo
2 wt.% Ni/5CeαAl$_2$O$_3$	N/A	700	1.0	46.5	*et al.*,
2 wt.% Ni/4Ce1ZrαAl$_2$O$_3$	N/A	700	1.0	66	(2009)
2 wt.% Ni/2.5Ce2.5ZrαAl$_2$O$_3$	N/A	700	1.0	55	
2 wt.% Ni/1Ce4ZrαAl$_2$O$_3$	N/A	700	1.0	57	
2 wt.% Ni/5ZrαAl$_2$O$_3$	N/A	700	1.0	50	
3 wt.% Ni/Ce-ZrO$_2$	N/A	750	3.0	58.1	Dong *et*
10 wt.% Ni/Ce-ZrO$_2$	N/A	750	3.0	89.2	*al.*,
15 wt.% Ni/Ce-ZrO$_2$	N/A	750	3.0	97	(2002)
20 wt.% Ni/Ce-ZrO$_2$	N/A	750	3.0	84.7	
30 wt.% Ni/Ce-ZrO$_2$	N/A	750	3.0	60.9	
15 wt.% Ni/Ce-ZrO$_2$	0.05	750	3.0	97	Roh *et*
15 wt.% Ni/ZrO$_2$	0.05	750	3.0	77	*al.*,
15 wt.% Ni/CeO$_2$	0.05	750	3.0	55	(2002)
15 wt.% Ni/MgAl$_2$O$_4$	0.05	750	3.0	79	
15 wt.% Ni/Al$_2$O$_3$	0.05	750	3.0	57	

[a] Time on steam of 2.0 h.

[b] Time on steam of 4.0 h.

[c] Nanocomposite Ni/ZrO$_2$

[d] Conventional zirconia

[e] Commercial alumina

3.2 Dry methane reforming

Dry methane reforming has a main problem from deactivation of catalyst. Several researchers investigated the effect of metal content (San-José-Alonso *et al*., 2009; Li *et al*., 2004), the effect of type of support (Li *et al*., 2011; Barroso-Quiroga *et al.*, 2010), and the effect of catalyst preparation to decrease the carbon or coke deposition that are shown in equation (2.3) - (2.4).

For example, the effect of metal content such as Ni and Co for dry methane reforming was investigated via San-José-Alonso *et al*., (2009). They studied Ni and Co metal loading to reduce the deactivation of catalyst. The catalysts were prepared by excess volume impregnation over a pelletized γ-alumina as a support. The operating conditions were temperature of 700 °C, 0.18 g of catalyst, a gas mixture $CH_4:CO_2$ (1:1, 60 ml/min), a space velocity of 22,000 h^{-1}, and the reaction time for 6 hours. The catalysts were reduced by H_2 (40 ml/min) at 500 °C for 90 min. The results showed that the best Ni and Co contents were 1 wt.% and 8 wt.% of Ni and Co, respectively and pure cobalt content of 9 wt.% which showed highest CH_4 conversion of 72 and 75 % at 30 min, respectively. But they had much carbon deposition of 268 $mg/g_{catalyst}$ and 290 $mg/g_{catalyst}$ for Ni-Co (1-8) and Co (9), respectively. Moreover, Cheng *et al*., (2010) investigated Ni and Co over Mo_2C as a support. Amounts of Ni and Co were varied from 0, 0.1, 0.2, 0.3, 0.4 and 0.5 molar ratios. The operating conditions were temperature of 850 °C, and a stoichiometric mixture ($CH_4:CO_2$ = 1:1) was fed at a flow rate of 40 ml/min with gas hourly space velocity (GHSV) of 3,800 h^{-1}. The Ni and Co were optimized for molybdenum carbides that were Ni/Mo ratio of 0.2 and Co/Mo ratio of 0.4. The best catalysts were $Ni_{0.2}Mo_1C_x$ and $Co_{0.4}Mo_1C_x$ which exhibited 89.2 % of CH_4 conversion for 120 min and 89.8 % of CH_4 conversion for 120 min without any deactivation, respectively.

The effects of supports for dry methane reforming were investigated via several researchers; for example, Barroso-Quiroga *et al.*, (2010) investigated Al_2O_3, CeO_2, ZrO_2, and La_2O_3 as support for CO_2 reforming of methane. The operating conditions were temperature of 600 °C, $CO_2:CH_4$ of 1:1, catalyst of 0.1 g, and reduction temperature of 600 K for 2.5 hours. 10 wt.%. Ni loading over CeO_2 and

ZrO_2 exhibited high maximum CH_4 conversion at 11.7 and 10.4 %, respectively. They offered higher CH_4 conversion than other supports. In addition, the CeO_2 showed the catalyst deactivation but ZrO_2 showed CH_4 conversion of 9.6 %. Furthermore, Li *et al*., (2004) and Li *et al*., (2011) investigated the mixing of supports between ZrO_2 and Al_2O_3. ZrO_2 showed the improvement of catalytic performance while Al_2O_3 showed high surface area that could improve the activity of catalyst. Li *et al*., (2004) studied the effect of support that was Al_2O_3-ZrO_2 and effect of Ni content on support that were synthesized by sol-gel method. The operating condition were temperature of 800 °C for 50 hours, hourly space velocity of 11,200 $mlg_{cat}^{-1}h^{-1}$, atmospheric pressure and CH_4:CO_2 = 1:1. $20Ni/Al_2O_3$-ZrO_2 was the best catalyst that showed excellent activity and stability with 91.9% CO_2 conversion and 82.9% CH_4 conversion over 50 hours at 800 °C. Furthermore, Addition of CeO_2 could improve the dispersion and enhanced the adsorption of CO_2 on the catalyst that was studied via Li *et al*., (2011). The effect of CeO_2 promoter over Al_2O_3-ZrO_2 as support and 10 wt.% Ni catalyst were investigated. The catalyst, supports and promoter were synthesized by sol-gel method. From the results, the addition of CeO_2 was more CO_2 conversion and CH_4 conversion than non-addition of CeO_2 about 92.2% and 80.1%, respectively.

Table 3.2 Summary of previous works with different catalysts, supports and conditions for dry methane reforming reaction.

Catalyst	Amount (g)	Condition		CH_4 Conversion (%)	Ref.
		Temp. (°C)	CH_4:CO_2		
(9)Ni/γ-Al_2O_3	0.18	700	1:1	54.0	San-José-Alonso *et al*., (2009)
(8)Ni(1)Co/γ-Al_2O_3	0.18	700	1:1	56.0	
(4.5)Ni(4.5)Co/γ-Al_2O_3	0.18	700	1:1	62.0	
(1)Ni(8)Co/γ-Al_2O_3	0.18	700	1:1	71.0	
(9)Co/γ-Al_2O_3	0.18	700	1:1	75.0	
5 wt.% Ni/Al_2O_3-ZrO_2	N/A	800	1:1	75.7	Li *et al*., (2004)
10 wt.% Ni/Al_2O_3-ZrO_2	N/A	800	1:1	77.0	
15 wt.% Ni/Al_2O_3-ZrO_2	N/A	800	1:1	81.1	

20 wt.% Ni/Al$_2$O$_3$-ZrO$_2$	N/A	800	1:1	82.9	
20 wt.% Ni/Al$_2$O$_3$	N/A	800	1:1	77.9	
10 wt.% Ni/Al$_2$O$_3$[a]	N/A	800	1:1	77.9	Li *et al.*, (2011)
10 wt.% Ni/Al$_2$O$_3$-ZrO$_2$[a]	N/A	800	1:1	76.7	
10 wt.% Ni/Al$_2$O$_3$-ZrO$_2$-CeO$_2$[a]	N/A	800	1:1	80.1	
10 wt.% Ni/γ-Al$_2$O$_3$[b]	N/A	800	1:1	-	
5 wt.% Ni/CZ100[c]	1.0	700	1:1	21	Kambolis *et al.*, (2010)
5 wt.% Ni/CZ75[c]	1.0	700	1:1	35	
5 wt.% Ni/CZ44[c]	1.0	700	1:1	31	
5 wt.% Ni/CZ28[c]	1.0	700	1:1	39	
5 wt.% Co/SiO$_2$	1.0	700	1:1	34	Bouarab *et al.*, (2004)
5 wt.% Co/(5)MgO-SiO$_2$	1.0	700	1:1	76	
5 wt.% Co/(10)MgO-SiO$_2$	1.0	700	1:1	60	
5 wt.% Co/(35)MgO-SiO$_2$	1.0	700	1:1	80	
10 wt/% Ni/α-Al$_2$O$_3$	0.1	600	1:1	8.4	Barroso-Quiroga *et al.*, (2010)
10 wt/% Ni/CeO$_2$	0.1	600	1:1	11.7	
10 wt/% Ni/La$_2$O$_3$	0.1	600	1:1	4.4	
10 wt/% Ni/ZrO$_2$	0.1	600	1:1	10.4	
10 wt/% Ni-Li/CeO$_2$	0.1	600	1:1	3.0	
10 wt/% Ni-K/CeO$_2$	0.1	600	1:1	3.5	
2Mg/Al[d]	0.2	800	1:1	0.1	Djaidja *et al.*, (2006)
(0.05)Ni(0.95)Mg[d]	0.2	800	1:1	1.1	
(0.05)Ni(0.95)Al[d]	0.2	800	1:1	96.2	
5 wt.% Ni/MgO[b]	0.2	800	1:1	97.1	
2((0.05)Ni(0.95)Mg)/Al[d]	0.2	800	1:1	97.2	
2((0.10)Ni(0.90)Mg)/Al[d]	0.2	800	1:1	97.5	

[a] Prepared by a sol-gel method

[b] Prepared by an impregnation method

[c] CZXX, where XX is % molar content of ceria and zirconia respectively.

[d] Prepared by a co-precipitation method

3.3 Biogas steam reforming

Araki *et al*., (2009) studied start-up procedures in autothermal reforming of biogas over 30 wt.% Ni based catalytic monolith. Figure 3.1 indicates schematic diagram of the apparatus. Initial feed temperature of oxygen and steam was varied. Initial feed oxygen temperature between 25 and 400 °C exhibited high CH_4 conversion (98.4-98.8 % CH_4 conversion) at steam temperature of 627 °C and initial feed steam temperature of 25-350 °C exhibited low CH_4 conversion (0 % conversion of CH_4) but at initial feed steam temperature of 450 – 550 °C exhibited high CH_4 conversion (97.9-98.3 % CH_4 conversion) at oxygen temperature of 25 °C.

Kolbitsch *et al*., (2008) investigated catalytic steam reforming of model biogas. The compositions of biogas were 60 % of CH_4 and 40 % of CO_2. The physicals properties were diameter of 14 mm, length of 19 mm and S_{BET} of 12 m^2/g. The chemical composition of the catalyst were 18 wt.% of NiO, <0.1 wt.% of SiO_2, <0.05 wt.% and CaO/Al_2O_3 as a support. They investigated the effects of temperature and steam to methane ratio (S/C). The results indicated that the optimal temperature of 750 °C and the CH_4 conversion increased with increasing the steam to methane ratio. However, high S/C required high energy to evaporate the excess water.
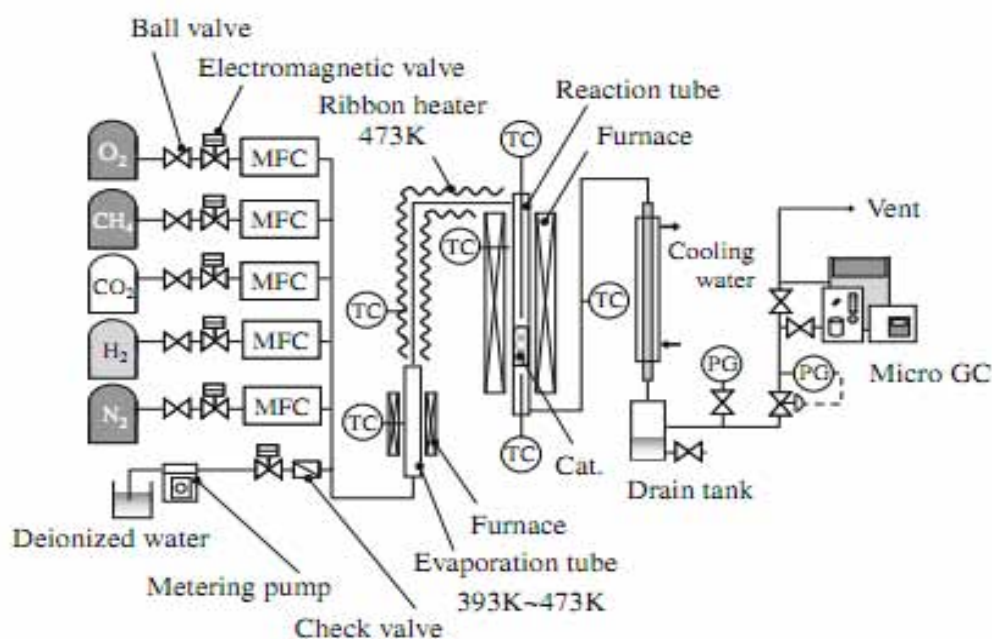
Figure 3.1 Schematic diagrams of the apparatus. (Araki *et al*., 2009)

3.4 Sorption enhanced steam methane reforming

Steam methane reforming process can improve the hydrogen yield via the use of adsorbent into a reactor for adsorption of a by-product as carbon dioxide and thus increasing product as hydrogen. Usually, researchers used hydrotalcite (Reijers *et al*., (2006); Oliveira *et al*., (2008)), dolomite (Hildenbrand *et al.,* 2006), calcium oxide (Martavaltzi *et al*., 2010), and lithium zirconate (Ochoa-Fernández *et al*., 2007) for carbon dioxide adsorption. For example, Hildenbrand *et al.,* (2006) investigated sorbent enhanced steam reforming (SESR) of methane using natural dolomite as carbon dioxide sorbent. The natural dolomite ($Ca_{0.5}Mg_{0.5}CO_3$) contained 0.05 wt.% Al, <10 ppm of other elements such as Cu, Ni, Zn, V, Cr and Co, and <1 ppm of heavy metals such as Pb, Cd and Hg. The $NiO/NiAl_2O_4$ catalyst was prepared by sol-gel method that was described by Ishida *et al.,* (2002). The catalysts were pretreated in air at 900 °C to convert $MgCa(CO_3)_2$ to MgO-CaO and reduced under 10% hydrogen in nitrogen at 900 °C for 1 h. The schematic drawing of the high pressure fluidized bed reactor is shown in Figure 3.2. The ratios of steam to carbon were investigated at a range of 2-4 and it had been found that the steam to carbon ratios of 4 gave the highest hydrogen yield. Furthermore, the intermediate at varies time on stream was analyzed via XRD. The XRD results exhibited peak of calcium hydroxide ($Ca(OH)_2$) and calcium carbonate ($CaCO_3$). These results could be explained that the formation of $Ca(OH)_2$ was occurred from the reaction of calcium oxide with steam as shown in equation (3.1), and $CaCO_3$ was formed by the reaction between calcium oxide and carbon dioxide as shown in equation (3.2). The experimental results indicated that higher than 90% H_2 was obtained when using dolomite as adsorbent and 60% H_2 was exhibited when not using dolomite.
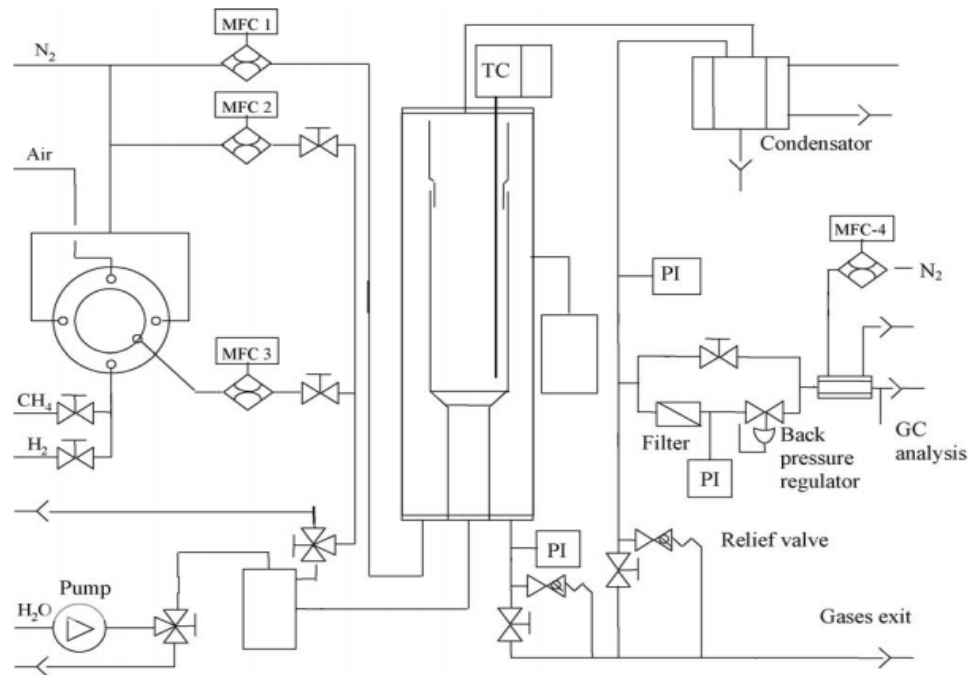
Figure 3.2 The schematic drawing of the high pressure fluidized bed reactor (Hildenbrand *et al.,* 2006)

$$H_2O + CaO \leftrightarrow Ca(OH)_2 \qquad \Delta H_{298}^0 = \text{-109 kJ/mole} \qquad \dots (3.1)$$

$$CO_2 + CaO \leftrightarrow CaCO_3 \qquad \Delta H_{298}^0 = \text{-179 kJ/mole} \qquad \dots (3.2)$$
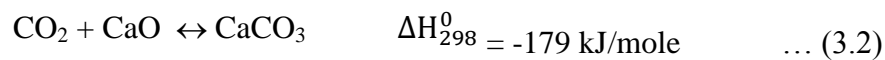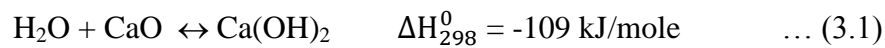
Moreover, CO_2 sorption on hydrotalcite and alkali-modified by K ad Cs at high temperature (403 °C) was investigated via Oliveira *et al*., (2008). Three hydrotalcites with different Mg/Al ratios were studied for CO_2 adsorption. The two alkali metals (including K and Cs) were impregnated over hydrotalcites. The results showed that the highest CO_2 sorption capacity (0.76 mmol/g) was given from using MG30-K and the small capacity was lost after 75 sorption/desorption cycles. Table 3.3 shows comparison of CO_2 sorption capacity.

Table 3.3 Comparison of CO_2 sorption capacity of different composition of hydrotalcites.

Adsorbent	t_{bt} (min)	q (mmol/g)	Ref.
MG30		0.09	Oliveira *et al*., (2008)
MG30-K		0.76	
MG30-Cs		0.44	
MG50		0.10	
MG50-K	N/A	0.59	
MG50-Cs		0.34	
MG70		0.12	
MG70-K		0.52	
MG70-Cs		0.41	
PURAL MG70	7.5	0.14[a]	Reijers *et al*., (2006)
PURAL MG61 HT	8.8	0.18[a]	
PURAL MG50	7.9	0.17[a]	
PURAL MG30	12.5	0.29[a]	
ECN-HTC	9.0	0.18[a]	

[a] CO_2 adsorbed up to the breakthrough time t_{bt}

Recently, Martavaltzi and co worker (2010) investigated steam reforming of methane with carbon dioxide capture over $CaO-Ca_{12}Al_{14}O_{33}$ as a sorbent. The calcium oxide was prepared by calcium acetate as a precursor and calcined at 850 °C for 1 h. The $CaO-Ca_{12}Al_{14}O_{33}$ was prepared by mixing aluminum nitrate enneahydrate $(Al(NO_3)_3.9H_2O)$ and calcium oxide in distilled water to achieve weight of $CaO:Ca_{12}Al_{14}O_{33}$ equal to 85:15. The catalyst was reduced at 850 °C for 1 h in a 30% H_2/He flow. 1.5 g of catalyst and 3 g of sorbent were added in the reactor. The sorbent was regenerated in 100% He flow at 850 °C. The experimental results indicated 93% conversion of methane at 650 °C, 1 bar and steam to methane molar ratio of 3.4. For sorption enhance steam reforming process, the purity of hydrogen was shown in outlet stream (>92%) but the conventional steam reforming exhibited only 77% hydrogen concentration in outlet stream. Moreover, the hydrogen concentration showed stable

for 13th cycles. In addition, the comparison between stoichiometric capacity (%) and experiment capacity of CaO, Li_2ZrO_3, $K-Li_2ZrO_3$, Na_2ZrO_3 and Li_4SiO_4 is shown in Table 3.4. From Table 3.4, it had been found that CaO had the highest CO_2 adsorption capacity.

Table 3.4 Comparison between stoichiometric capacity and experiment capacity of alkali metals.

Adsorbent	Stoichiometric Capacity[a] (%)	Experiment Capacity[a] (%)	Ref.
CaO	78.6	49.5	Ochoa-
Li_2ZrO_3	28.8	27.1	Fernández *et*
$K-Li_2ZrO_3$[b]	26.6	20.7	*al*., (2007)
Na_2ZrO_3	23.4	16.3	
Li_4SiO_4	36.6	22.9	

[a] Capacity is $(g_{CO2}/g_{acceptor})$ x 100

[b] K:Li:Zr is 0.2:2.2:1

Furthermore, Hydrogen production via sorption enhanced steam methane reforming using nickel over calcium oxide multifunctional catalyst was investigated by Chanburanasiri *et al*., (2012). They found that 12.5 wt.% Ni/Al_2O_3 mixed with CaO exhibited the highest CH_4 conversion (89%) when compared with 12.5 wt.% Ni/CaO (86%) and 12.5 wt.% Ni/Al_2O_3 (84%, without CO_2 sorption effect). Moreover, the 12.5 wt.% Ni/Al_2O_3 mixed with CaO showed the highest purity of hydrogen (83%) when compared with 12.5 wt.% Ni/CaO (82%), 12.5 wt.% Ni/MG30-K (75%), and 12.5 wt.% Ni/Al_2O_3 (72%).

CHAPTER IV

EXPERIMENTAL

This chapter provides details of chemicals and gases used in the experiments, catalyst preparation method (incipient wetness impregnation), CO_2 adsorption test, and reaction test of sorption enhanced biogas steam reforming process.

4.1 Chemicals and gases

1. Commercial alumina (Al_2O_3, Sigma Aldrich)
2. Calcium oxide (CaO, Riedel-deHaen)
3. Nickel nitrate hexahydrate ($Ni(NO_3)_2 \cdot 6H_2O$, Sigma Aldrich)
4. Silicon carbide (SiC, Sigma Aldrich)
5. Nitrogen gas 99.999% (N_2)
6. Methane 99.999% (CH_4)
7. Carbon dioxide 99.999% (CO_2)
8. Deionized water

4.2 Catalyst preparation

The alumina commercial support and calcium oxide were used as support for CO_2 sorption testing and sorption enhanced biogas steam reforming process. Nickel nitrate hexahydrate (Aldrich) was used as precursor for impregnation on support. Firstly, $Ni(NO_3)_2 \cdot 9H_2O$ was dissolved by Deionized water to obtain Ni solution. After that, Ni solution was dropped on alumina and calcium oxide. Then, they were dried at 100 °C over night and calcined at 800 °C for 4 h. Figure 4.1 shows the step of catalyst synthesis.
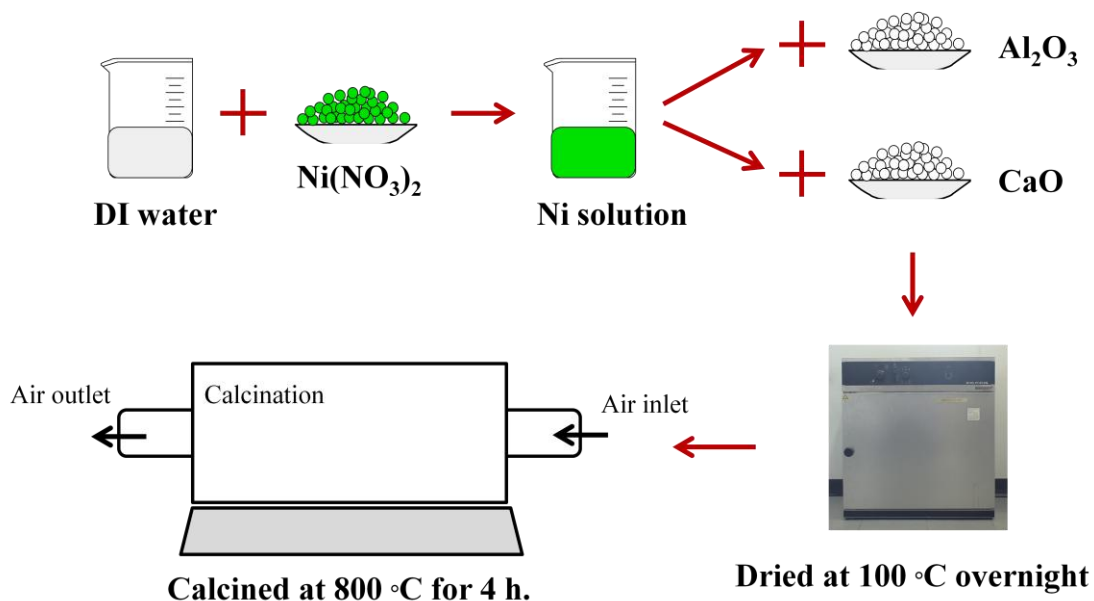
Figure 4.1 Step of catalyst synthesis by incipient wetness impregnation method

4.3 Adsorption testing

Calcium oxide (CaO) was used as an adsorbent. 2 g of CaO and 1.5 g of SiC were mixed and were packed into a fixed bed quartz reactor (ID of 10 mm, OD of 12 mm). The bottom and top of adsorbent were packed with quartz wool of 1 and 0.5 g, respectively. They were pretreated at 750 °C with N_2 (50 ml/min) for 60 min. Then, 8% CO_2 in N_2 total flow rate of 50 ml/min was fed into the reactor for CO_2 adsorption testing at atmospheric pressure and various temperatures (450, 500, 550 and 600 °C). In addition, for the study on the effect of feed steam, 8% CO_2 was mixed with steam and fed into the reactor for CO_2 sorption testing with steam. Then, the water in the effluent was trapped with ice bath and analyzed by gas chromatograph (Shimadzu GC-8A equipped with Molecular Sieve and Poraplot column).

4.4 Catalytic performance

The sorption enhanced biogas steam reforming reaction was tested in the fixed bed quartz reactor (ID of 10 mm, OD of 12 mm and length of 500 mm). 0.8 g of catalysts (12.5 wt.% Ni/Al$_2$O$_3$ and 12.5 wt.% Ni/CaO) and 2 g of adsorbent (CaO)

were packed and supported by quartz wool. Types of bed arrangement were investigated as shown in Figure 4.2.
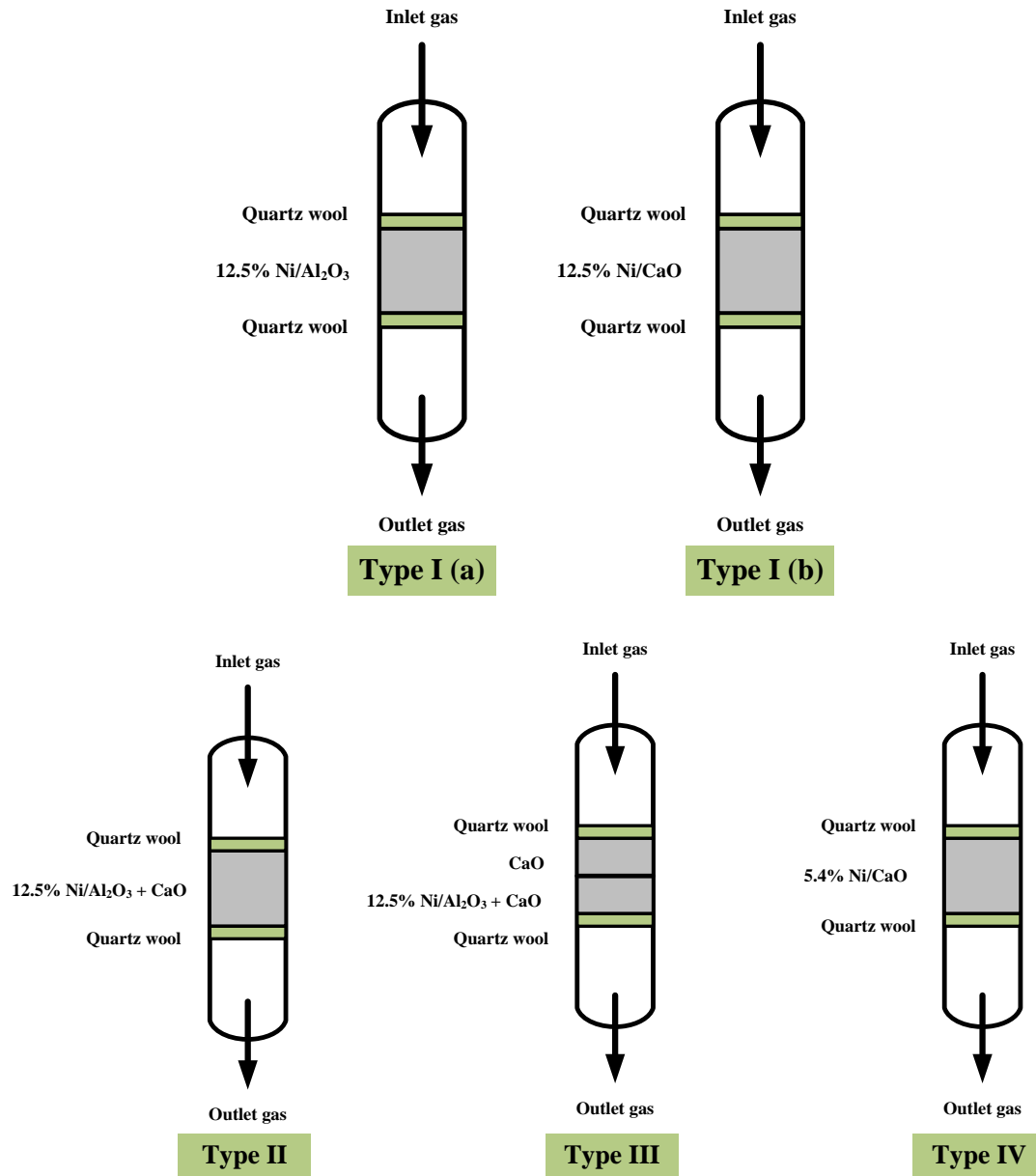
Figure 4.2 Types of bed arrangement for sorption enhanced biogas steam reforming testing

Four systems of bed arrangement were packed in the fixed-bed quartz reactor. For the first system (a) and (b), 0.8 g of catalysts (12.5 wt.% Ni/Al_2O_3 and 12.5 wt.% Ni/CaO) were mixed with 6 g of SiC. For the second system, 0.8 g of catalyst (12.5 wt.% Ni/Al_2O_3) was mixed with 2 g of adsorbent (CaO) and packed in the reactor. The third system, two stage of bed was separated, top consisting 1 g of CaO and bottom consisting 0.8 g of 12.5 wt.% Ni/Al_2O_3 mixed with 1 g of CaO. For the fourth system, a suitable amount of adsorbent was loaded with Ni with the equivalent amount of Ni used in the study of Type I. All of systems were filled with SiC as diluent. The catalysts were pretreated at 750 °C for 1 h with N_2 (25ml/min) and reduced at 750 °C for 1.5 h with 50% H_2 in N_2 (total flow rate 50 ml/min). Figure 4.3 shows the setup of the sorption enhanced biogas steam reforming system. The reactions were tested at reaction temperature of 600 °C. The total flow rate of inlet stream was 50 ml/min. The CH_4 to CO_2 ratio was 1.5 and S/C ratio was 3. The product stream was trapped by an ice bath and analysed by gas chromatography (GC-8A, shimazu) equipped with two columns that were Molecular Sieve and Poraplot. Table 4.1 shows the details and conditions of gas chromatography.
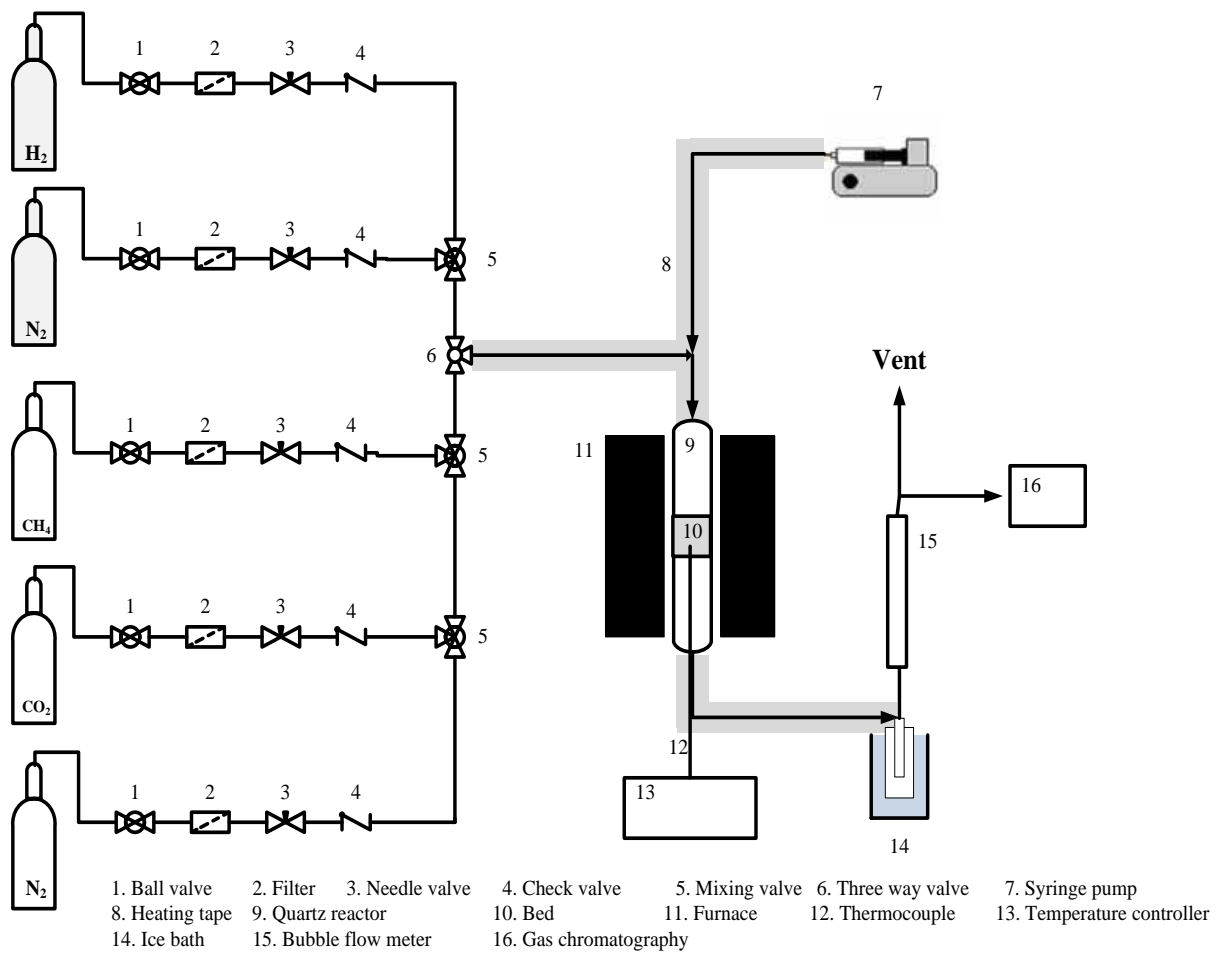
Figure 4.3 Experimental equipments for hydrogen production via sorption enhanced biogas steam reforming study

Table 4.1 Operating conditions for gas chromatography

Gas Chromatography	Shimadzu GC-8A	
Detector	TCD	
Column	Molecular sieve 5A	Porapak-Q
- Column material	SUS	SUS
- Length (m)	2	2
- Outer diameter (mm)	4	4
- Inner diameter (mm)	3	3
- Mesh range	60/80	60/80
- Maximum temperature (˚C)	350	350
Carrier gas	Ar (99.999%)	Ar (99.999%)
Carrier gas flow (ml/min)	30	30
Column temperature		
- initial (˚C)	50	50
- final (˚C)	50	50
Injector temperature (˚C)	70	70
Detector temperature (˚C)	100	100
Current (mA)	70	70
Analyzed gas	N_2, H_2, CO, CH_4	CO_2

4.5 Catalyst characterization

1. X-ray diffraction (XRD)

X-ray diffraction (XRD) was used for catalyst characterization. XRD pattern was determined by D8 Advance of Bruker AXS, equipping with long fine focus ceramic as X-ray source (using Cu K_α source). The pattern was recorded in range of $10° < 2\theta < 80°$ with an increasing step of $0.04°$, wavelength 1.54056 nm and scan speed of 0.5.

2. N$_2$ adsorption desorption

The surface area of catalyst and adsorbent was measured by using N$_2$ adsorption desorption technique. They were carried out by using Micromeritics Chemisorp 2750. The nitrogen adsorption desorption isotherms was tested at 77 K with 0.2 g of catalyst.

CHAPTER V

RESULTS AND DISCUSSION

This chapter presents thermodynamic analysis of biogas steam reforming process, CO_2 adsorption of CaO with/without presence of steam at different temperatures and experimental study on the sorption enhanced biogas steam reforming process.

5.1 Thermodynamic analysis

A reformer is a unit that is used for biogas steam reforming reaction. Biogas steam reforming reaction involves steam methane reforming (SMR, Equation 5.1), dry methane reforming (DMR, Equation 5.2) and water gas shift reaction (WGSR, Equation 5.3). Biogas steam reforming was simulated via Aspen Plus program. It was assumed that the thermodynamic equilibrium was achieved and determined by Gibbs free energy minimization. NRTL Equation of State was used in the thermodynamic calculation. Gases have been fed into the reactor (Figure 5.1, atmospheric pressure, CH_4/CO_2 of 1.5 and S/C of 3).

$$CH_4 + H_2O \leftrightarrow 3H_2 + CO \qquad \Delta H^0_{298} = +206 \text{ kJ/mol} \qquad \dots (5.1)$$

$$CH_4 + CO_2 \leftrightarrow CO + H_2 \qquad \Delta H^0_{298} = +247 \text{ kJ/mol} \qquad \dots (5.2)$$

$$CO + H_2O \leftrightarrow H_2 + CO_2 \qquad \Delta H^0_{298} = -41.1 \text{ kJ/mol} \qquad \dots (5.3)$$
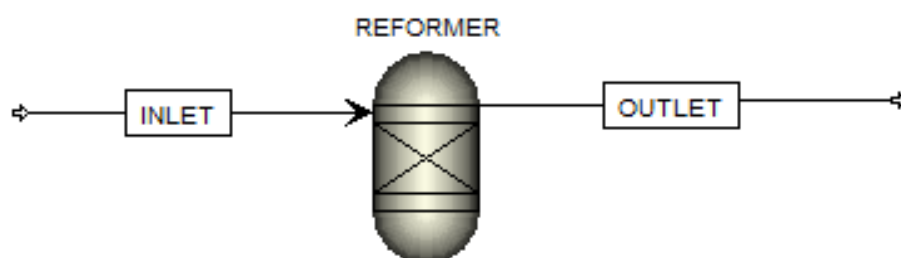

Figure 5.1 Process flow diagram for biogas steam reforming.

Normally, steam methane reforming and dry methane reforming are highly endothermic reactions, so high CH_4 conversion can be achieved when operating the reaction at high temperature. Figures 5.2 and 5.3 show outlet product gases compositions (%) from the reactor including CH_4, CO_2, H_2 and CO, and CH_4 conversions at different temperatures (range of temperature is 400-800 °C). The results indicated that temperatures above of 600 °C showed high H_2 concentration (65 %) and CH_4 conversion (98 %) that was nearly 100 % and, therefore, at higher temperatures it became less attractive for operating the sorption enhanced biogas steam reforming to improve the CH_4 conversion. Moreover, high reaction temperature operation required expensive wall materials (Johnsen *et al.*, 2006) and was prone to deactivation of catalyst from coke formation and sintering (Solieman *et al.*, 2009). Not only equilibrium CH_4 conversion and H_2 concentration are the factors to be of concern, but also suitable sorption temperature of adsorbents is an important for high performance of sorption enhanced process. Previous works have reported the stoichiometric capacity and experimental capacity of CaO, Li_2ZrO_3, $K-Li_2ZrO_3$, Na_2ZrO_3, and Li_4SiO_4 (Ochoa-Fernández *et al.*, 2007) as summarized in Table 5.1. CaO is an adsorbent which offers the highest CO_2 sorption capacity at 575 °C.
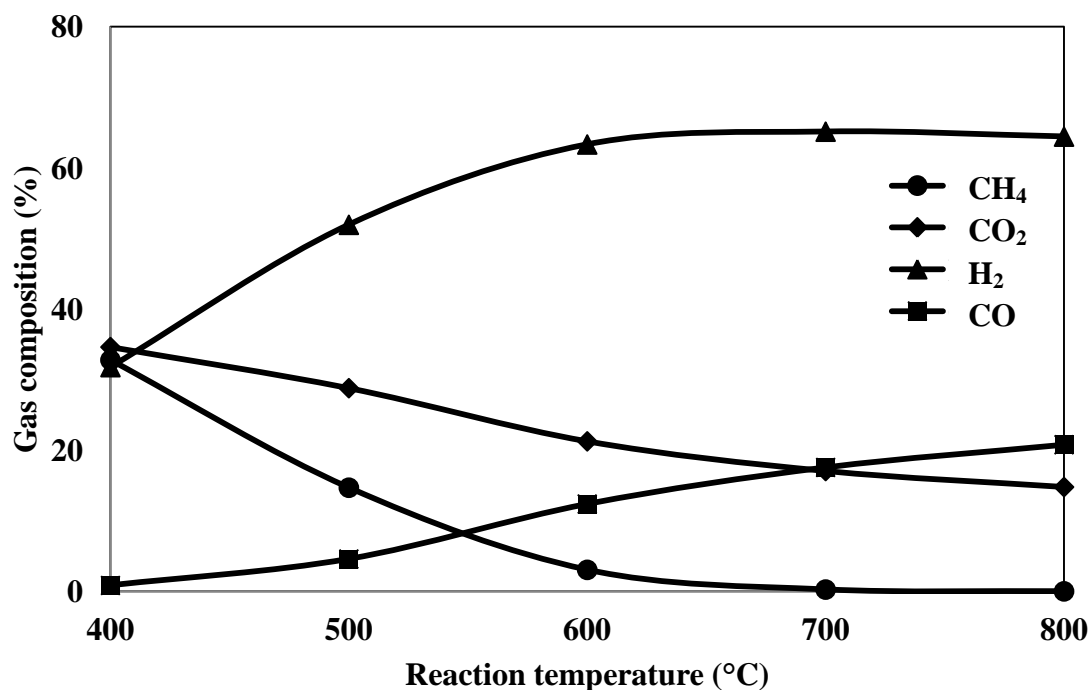
Figure 5.2 Outlet gases composition at different temperatures (atmospheric pressure, CH_4/CO_2 of 1.5 and S/C of 3)
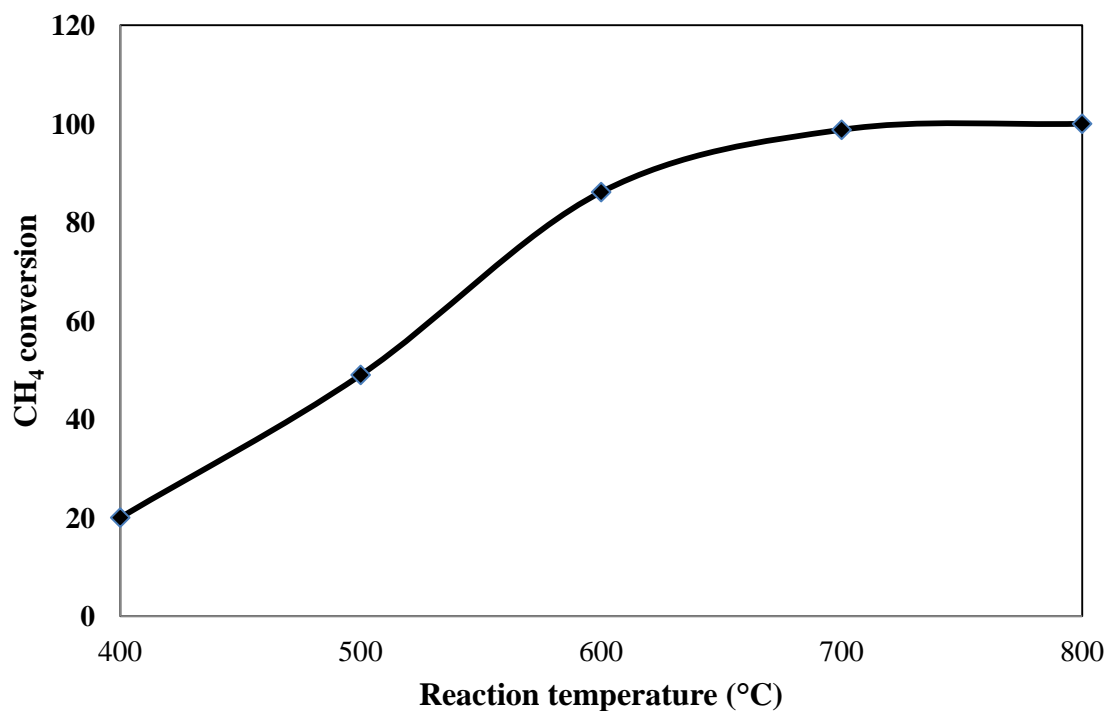
Figure 5.3 CH$_4$ conversions of biogas steam reforming at different temperatures (atmospheric pressure, CH$_4$/CO$_2$ of 1.5 and S/C of 3)

Table 5.1 Comparison CO$_2$ sorption between stoichiometric capacity and experiment capacity of alkali metals at 575 °C (Ochoa-Fernández *et al*., 2007).

Adsorbent	Stoichiometric capacity[a] (%)	Experiment capacity[a] (%)
CaO	78.6	49.5
Li$_2$ZrO$_3$	28.8	27.1
K-Li$_2$ZrO$_3$[b]	26.6	20.7
Na$_2$ZrO$_3$	23.4	16.3
Li$_4$SiO$_4$	36.6	22.9

[a] Capacity is (g$_{CO2}$/g$_{acceptor}$) x 100

[b] K:Li:Zr is 0.2:2.2:1

Therefore, in this study CaO was selected as a CO_2 acceptor and a range of temperature for sorption enhanced biogas steam reforming was optimized (i.e. 450, 500, 550 and 600 °C). Furthermore, two catalysts (12.5 wt.% Ni/Al_2O_3 and 12.5 wt.% Ni/CaO) were synthesized for this reaction by incipient wetness impregnation method. XRD patterns were measured for confirmation of catalyst and supports. The XRD pattern of 12.5 wt.% Ni/Al_2O_3 indicated peaks of NiO and Al_2O_3, while 12.5 wt.% Ni/CaO indicated peaks of NiO, CaO, $Ca(OH)_2$ and $CaCO_3$. They are shown in Figure 5.4. BET surface area was tested for all fresh catalysts and supports, and the results are shown in Table 5.2. The surface area was decreased when the nickel metal was loaded on the supports that because the nickel metal may block pore of supports, so the surface area was decreased.
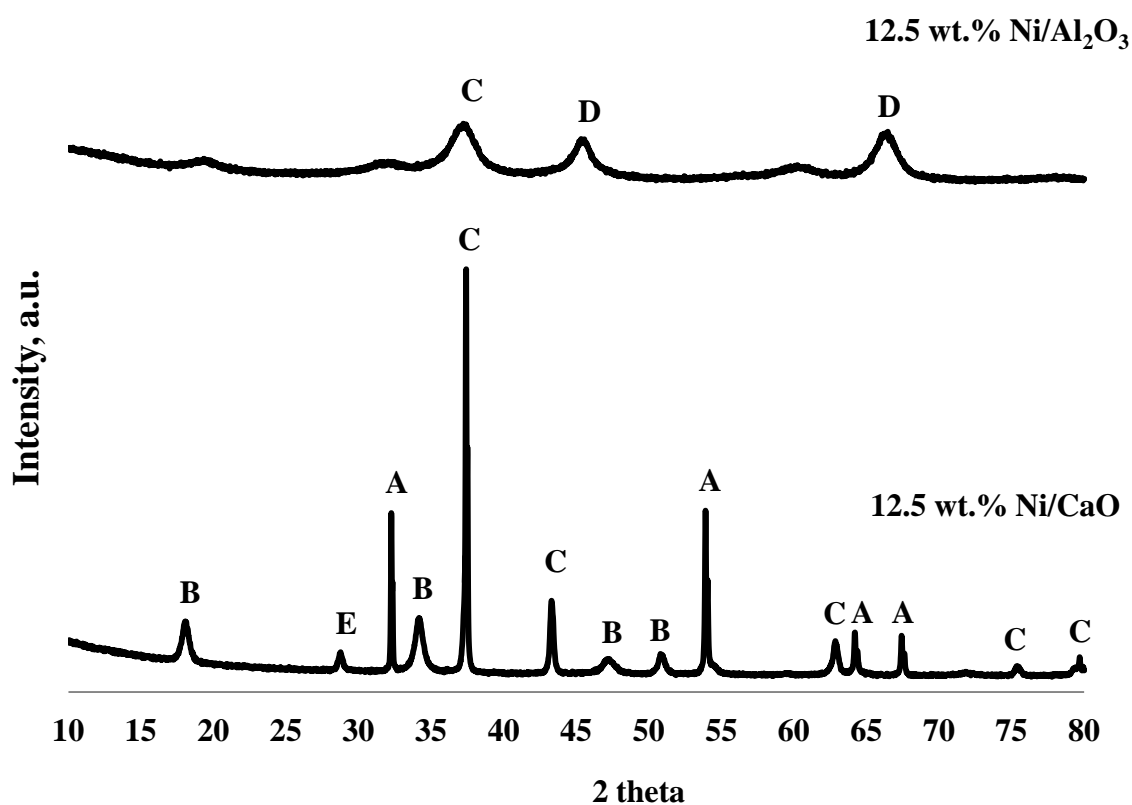

Figure 5.4 XRD patterns of 12.5 wt.% Ni/Al_2O_3 and 12.5 wt.% Ni/CaO (A: CaO, B: $Ca(OH)_2$, C: NiO, D: Al_2O_3, and E: $CaCO_3$)

Table 5.2 Surface area of fresh catalysts and supports

Catalyst	BET surface area (m^2/g)
Al_2O_3	99.52
12.5 wt.% Ni/Al_2O_3	53.12
CaO	1.92
12.5 wt.% Ni/CaO	1.11
SiC	0.49

5.2 Adsorption testing

Performance of CaO on CO_2 adsorption was tested in the fixed bed quartz reactor. 8% CO_2 in N_2 was fed into the reactor with a total flow rate of 50 ml/min. Effect of adsorption temperature, adsorption capacity of CaO supported catalyst, and effect of steam were investigated in this section.

5.2.1 Effect of adsorption temperature

Four adsorption temperatures (450, 500, 550 and 600 °C) were tested for CO_2 adsorption by CaO. The performance is shown in Figure 5.4. The results showed that the values of t_b were 24, 28, 36 and 50 min for temperatures of 450, 500, 550 and 600 °C, respectively. At the temperatures of 450 and 500 °C, no CO_2 was detectable before 30 min but at higher temperatures (550 and 600 °C), the values of c/c_F were 0.02 and 0.04 for temperatures of 550 and 600 °C, respectively. Therefore, the product stream of a low temperature was more purified than that of a high temperature.
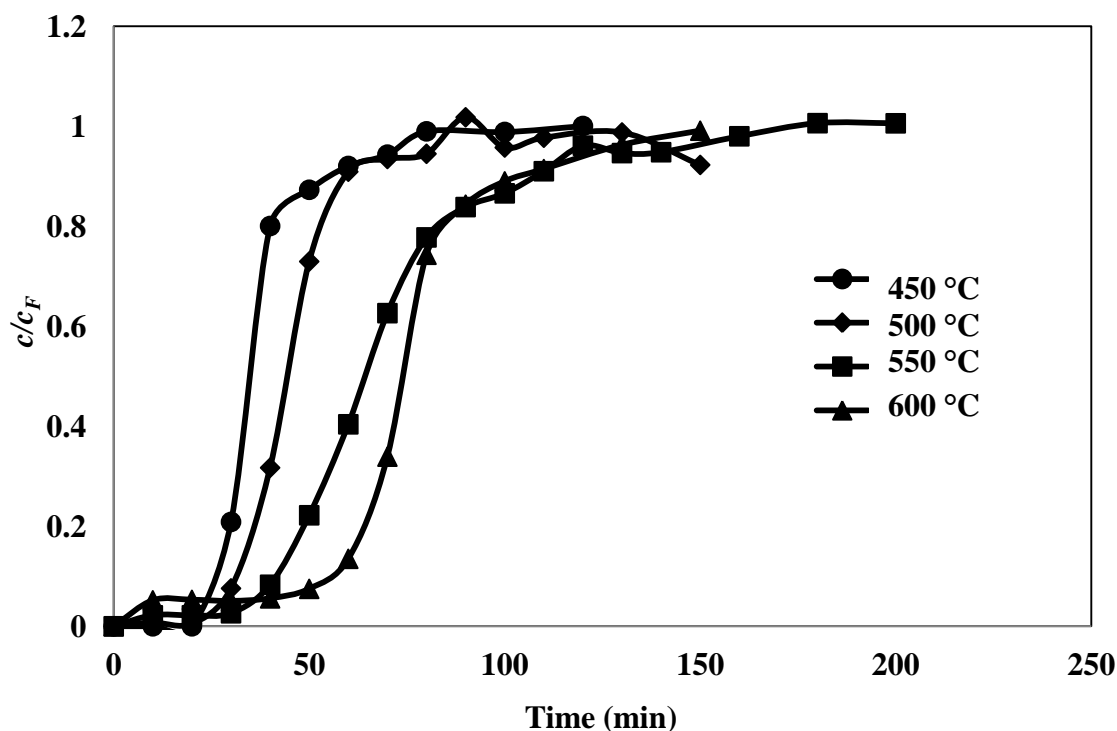
Figure 5.5 Breakthrough curves of CO_2 adsorption by CaO at different temperatures including 450, 500, 550 and 600 °C, atmospheric pressure and using 8% CO_2 in N_2 as feed composition

The CO_2 capacity for each adsorption temperatures are summarized in Table 5.3. The temperature of 600 °C showed the highest CO_2 capacity that was 0.2849 g_{CO2}/g_{CaO}. Therefore, in this study the temperature of 600 °C was chosen for sorption enhanced biogas steam reforming reaction.

Table 5.3 CO_2 adsorption capacity of CaO at different temperatures (450, 500, 550 and 600 °C)

Adsorption temperature (°C)	Experimental adsorption capacity ($g_{CO2}/g_{Adsorbent}$)
450	0.1427
500	0.1774
550	0.2503
600	0.2849

5.2.2 Adsorption capacity of CaO supported catalyst

Three types of adsorbent as supports of catalyst (CaO, 12.5 wt.% Ni/CaO and 12.5 wt.% Ni/Al$_2$O$_3$) were investigated for CO$_2$ adsorption at 600 °C. Figure 5.6 shows experimental results that t$_b$ of pure CaO, 12.5 wt.% Ni/CaO and 12.5 wt.% Ni/Al$_2$O$_3$ were 50, 30 and 2 min, respectively. Table 5.4 exhibits that pure CaO showed higher CO$_2$ adsorption (0.2849 g$_{CO2}$/g) than 12.5 wt.% Ni/CaO (0.1732 g$_{CO2}$/g) because amount of CaO in 12.5 wt.% Ni/CaO (1.75 g) was less than CaO (2 g). This is obviously that the presence of Ni metal hinders adsorption sites of CaO. Furthermore, it should be noted that CO$_2$ was not adsorbed over 12.5 wt.% Ni/Al$_2$O$_3$.
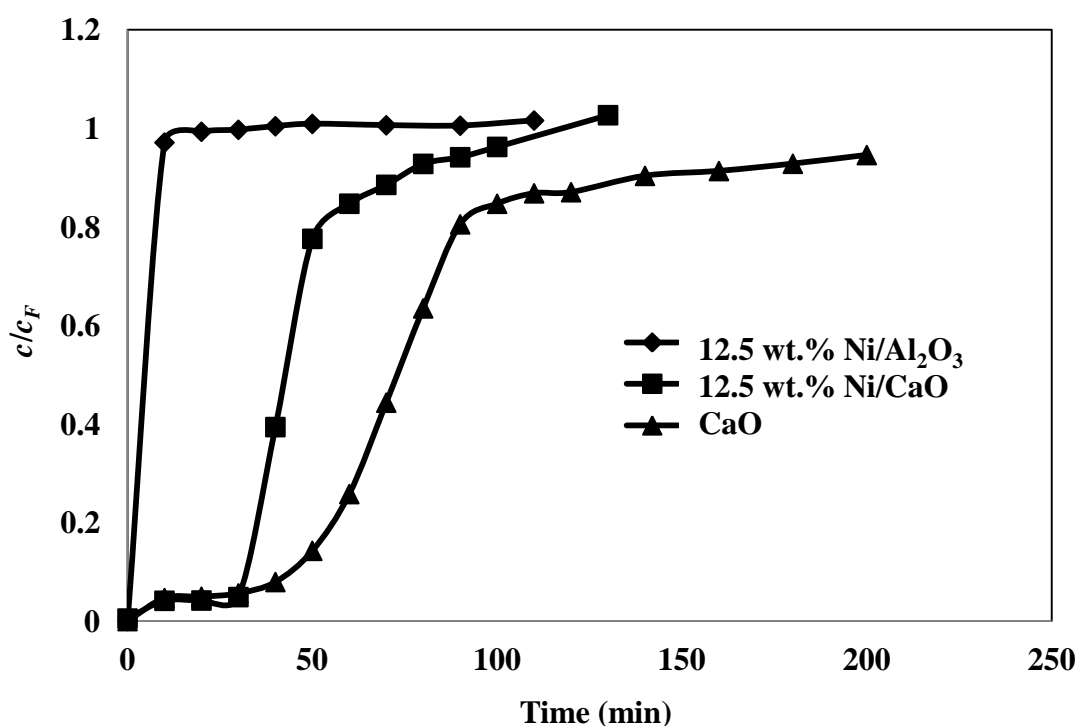

Figure 5.6 Breakthrough curve of CO$_2$ adsorption by CaO, 12.5 wt.% Ni/CaO and 12.5 wt.% Ni/Al$_2$O$_3$ at temperature of 600 °C, atmospheric pressure and using 8% CO$_2$ in N$_2$ as feed composition

Table 5.4 CO_2 adsorption capacity of CaO, 12.5 wt.% Ni/CaO and 12.5 wt.% Ni/Al_2O_3 at temperature of 600 °C)

Adsorbent	Adsorption temperature (°C)	Experiment adsorption capacity (g_{CO2}/g)
CaO	600	0.2849
12.5 Ni/CaO	600	0.1732
12.5 Ni/Al_2O_3	600	-

5.2.3 Effect of steam

Figure 5.7 shows the breakthrough curves from the adsorption test with and without the presence of steam. The results indicated that the presence of steam could enhance the CO_2 adsorption capacity of CaO. This is probably because the hydration of adsorbent (Equation 5.4) has effect of increasing adsorption capacity by increasing its porosity (Arias *et al*., 2010, Sun *et al*., 2008 and Blamey *et al*., 2011). Table 5.5 indicates that the CO_2 sorption capacity increases from 0.2849 g_{CO2}/g_{CaO} (without steam effect) to 0.6723 g_{CO2}/g_{CaO} when steam is added in the feed gas.

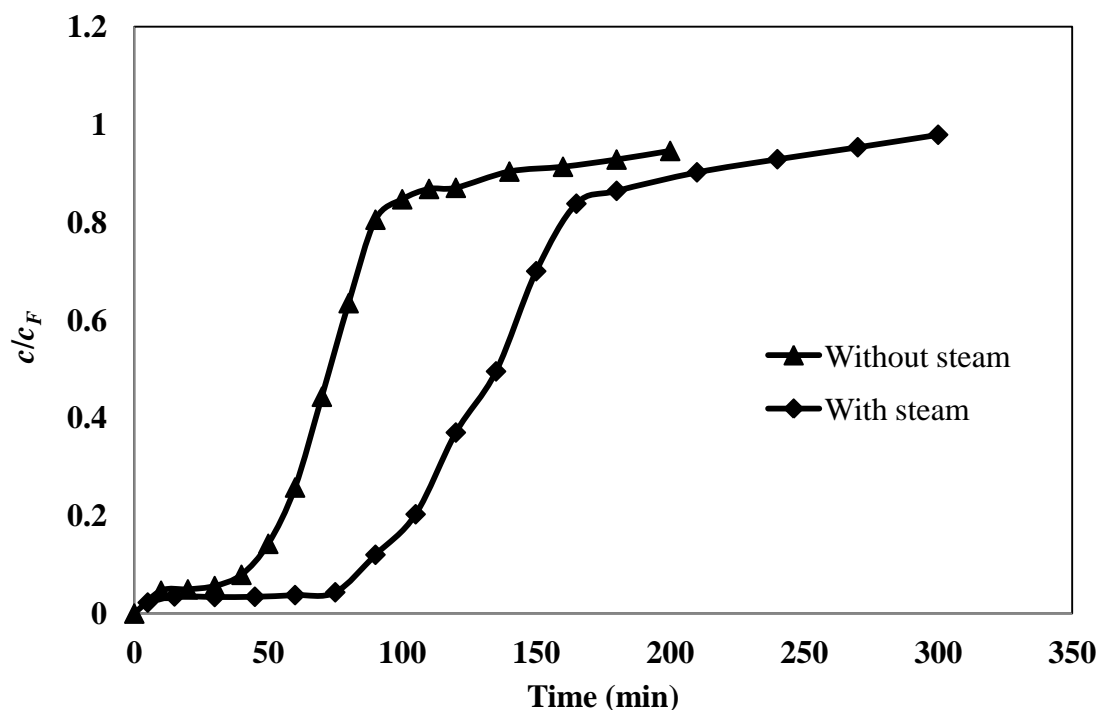$$Ca(OH)_{2(s)} + CO_{2(g)} \rightarrow CaCO_{3(s)} + H_2O_{(g)} \qquad \dots (5.4)$$

Figure 5.7 Breakthrough curve of CO_2 adsorption by CaO with and without feed steam that mixed with 8% CO_2 in N_2 as feed composition at temperature of 600 °C and atmospheric pressure

Table 5.5 CO_2 adsorption capacity of CaO with and without steam in feed at temperature of 600 °C and atmospheric pressure

Adsorbent	Adsorption temperature ($^{\circ}$C)	Experiment adsorption capacity ($g_{CO2}/g_{Adsorbent}$)
CaO with steam	600	0.6724
CaO without steam	600	0.2849

5.3 Sorption enhanced biogas steam reforming

Four types of bed arrangement were investigated for sorption enhanced biogas steam reforming. The feed with methane to carbon dioxide ratio (CH_4/CO_2) of 1.5 and steam to carbon ratio (S/C) of 3 was fed into the reactor. Reaction temperature and pressure were 600 °C and 1 atm, respectively. For Type I (a), 12.5 wt.% Ni/Al_2O_3 of

0.8 g mixed with SiC of 6 g were packed in the fixed bed reactor as shown in Figure 5.8 (a). The results indicated that the reaction reached steady state after 15 min (60% H_2, 20% CO_2, 15% CO and 5% CH_4) as shown in Figure 5.9. It should be noted from Table 5.4 that no adsorption of CO_2 on this catalyst was observed. Figure 5.10 shows that CH_4 conversion of 80% was exhibited for all experiments.
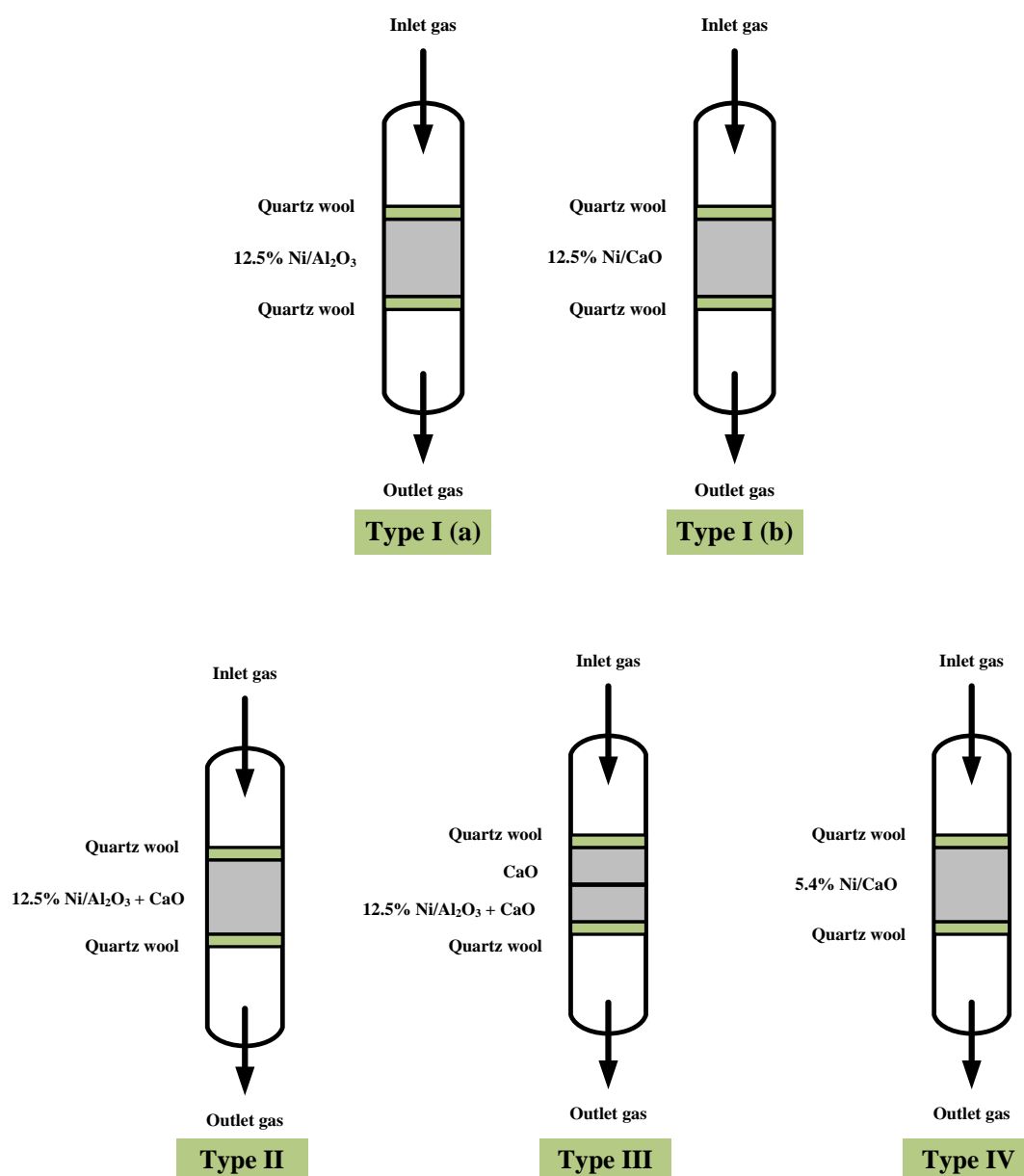

Figure 5.8 Types of bed arrangement for sorption enhanced biogas steam reforming
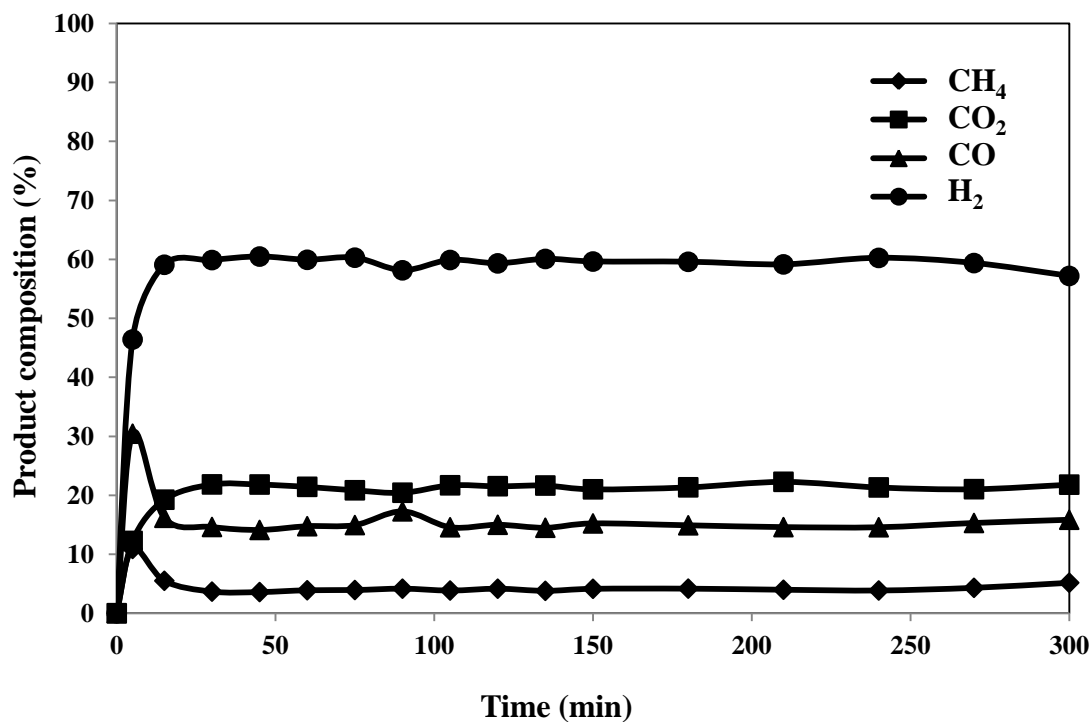
Figure 5.9 Gas product compositions (dry basis) of Type I (a) for sorption enhanced biogas steam reforming at S/C of 3, CH_4/CO_2 of 1.5, reaction temperature of 600 °C and atmospheric pressure

Figure 5.10 CH_4 conversion of Type I (a) for sorption enhanced biogas steam reforming at S/C of 3, CH_4/CO_2 of 1.5, reaction temperature of 600 °C and atmospheric pressure
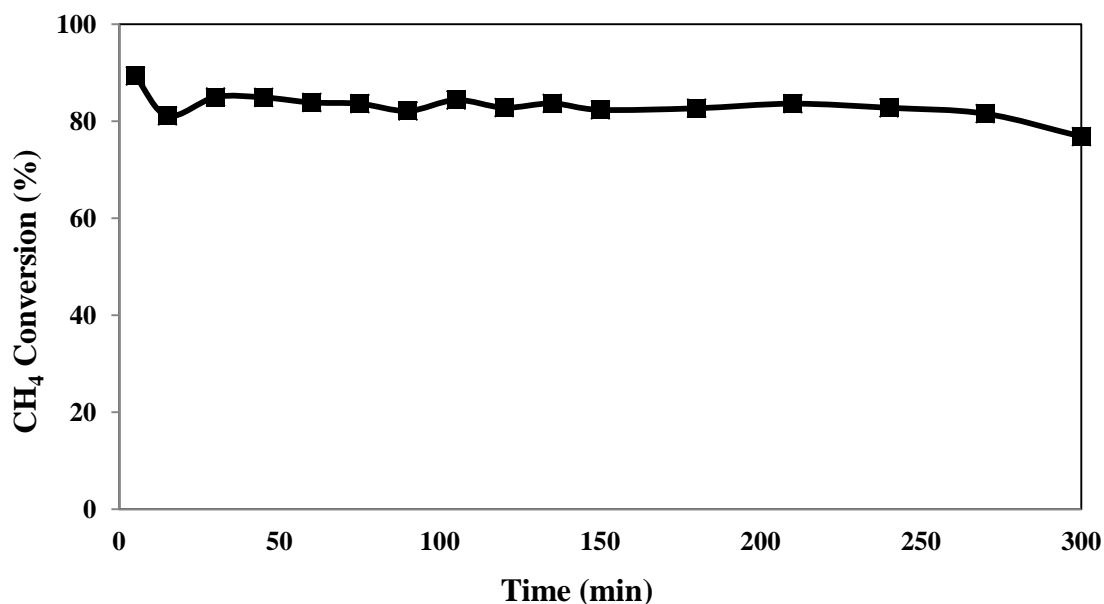
For type I (b), 12.5 wt.% Ni/CaO of 0.8 g and SiC of 6 g were packed in the fixed bed reactor as shown in Figure 5.8 (b). The results indicated that CO_2 was adsorbed by CaO at least before 30 min as the purity of hydrogen was high (80.7% H_2) (Figure 5.11). But after the adsorption period, the purity of hydrogen and CH_4 conversion decreased (42.6% H_2 and 28.8% CH_4 conversion at 300 min), indicating that the catalyst was deactivated. The change in the catalyst activity should be associated with the formation of $CaCO_3$ from the CO_2 adsorption on CaO during the reaction. Figure 5.13 shows the XRD patterns of the fresh and used 12.5 wt.% Ni/CaO catalysts. The XRD patterns indicated the presence of $CaCO_3$ occurred by CaO reacted with CO_2, $Ca(OH)_2$ likely from the reaction of CaO. When CaO reacted with CO_2 and became to $CaCO_3$, the volume of CaO was increased from 16.9 ml/g to 36.9 ml/g of $CaCO_3$ that means carbonation of CaO inside the pore generated a $CaCO_3$ and reduced the pore volume (Sultana and Chen, 2011). The reducing of pore volume had effect on decreasing of active site because some active site was in the pore and when pore volume was reduced that means pore may be blocked and active site was lost.

Figure 5.11 Gas product compositions (dry basis) of Type I (b) for sorption enhanced biogas steam reforming at S/C of 3, CH_4/CO_2 of 1.5, reaction temperature of 600 °C and atmospheric pressure

Figure 5.12 CH$_4$ conversion of Type I (b) for sorption enhanced biogas steam reforming at S/C of 3, CH$_4$/CO$_2$ of 1.5, reaction temperature of 600 °C and atmospheric pressure
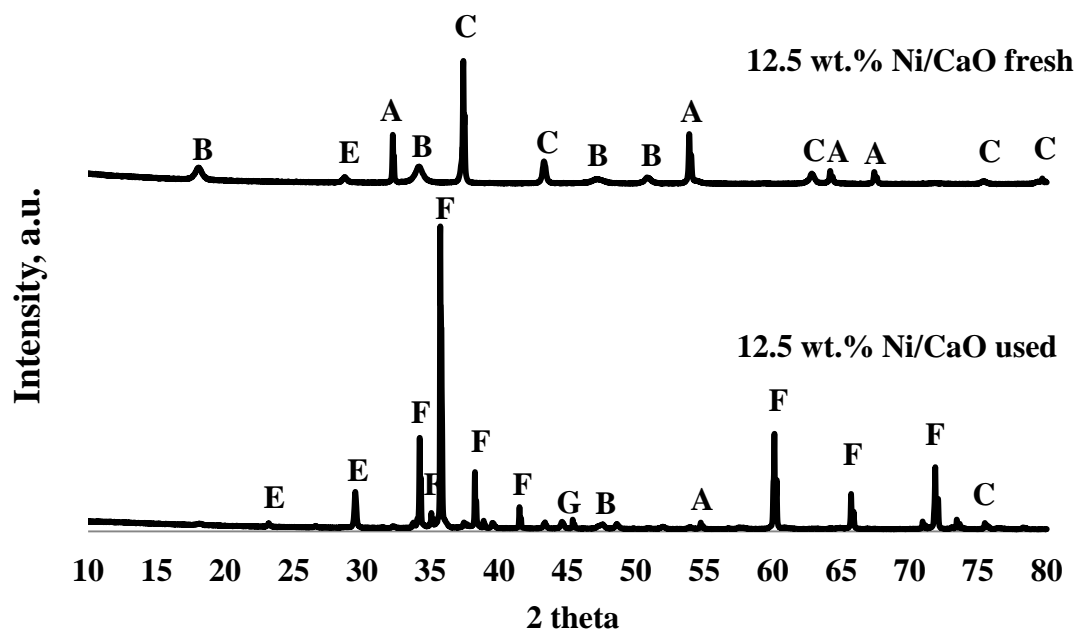
Figure 5.13 XRD patterns of fresh and used catalyst of 12.5 wt.% Ni/CaO (A: CaO, B: Ca(OH)$_2$, C: NiO, D: Al$_2$O$_3$, E: CaCO$_3$, F: SiC and G: Ni)

For operation in Type II configuration, 12.5 wt.% Ni/Al_2O_3 0.8 g mixed with CaO of 2 g and SiC of 1.5 g were packed in the fixed bed reactor (Figure 5.8 (Type II)). The purity of hydrogen and CH_4 conversion were increased by CO_2 adsorption. Before 30 min, CO_2 was adsorbed by CaO and became to $CaCO_3$. The purity of hydrogen was improved to 97.3% when compared with purity of hydrogen of 60% without the adsorption effect (Figure 5.14). Furthermore, maximum CH_4 conversion was increased to 93.7% when compared with CH_4 conversion of 80% at equilibrium without the CO_2 sorption effect as shown in Figure 5.15. The results showed that when CO_2 was adsorbed by CaO and became to $CaCO_3$, the hydrogen in production stream is purified and CH_4 conversion was improved. It should be noted that the reaction was forwarded by removal of a reaction product (CO_2) for this type of bed arrangement. Furthermore, for Al_2O_3 as a support there was no observed deactivation. At steady state with no effect from CO_2 adsorption, it was confirmed that the results agreed well with those from the experiment with only 12.5 wt.% Ni/Al_2O_3 in the study of Type I (a).
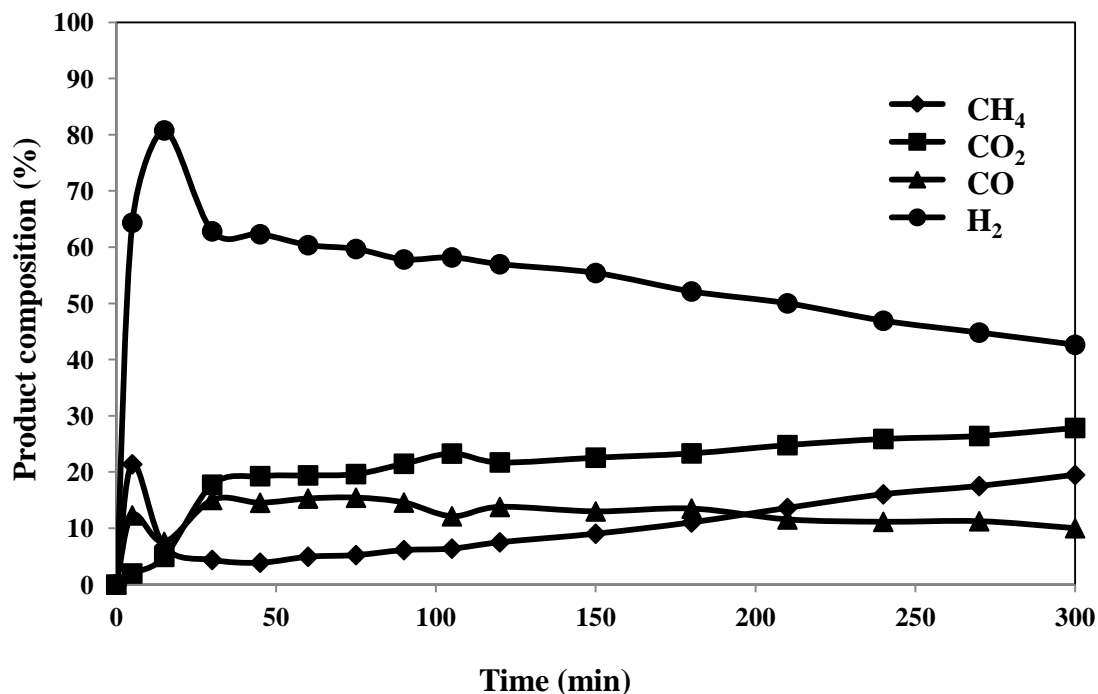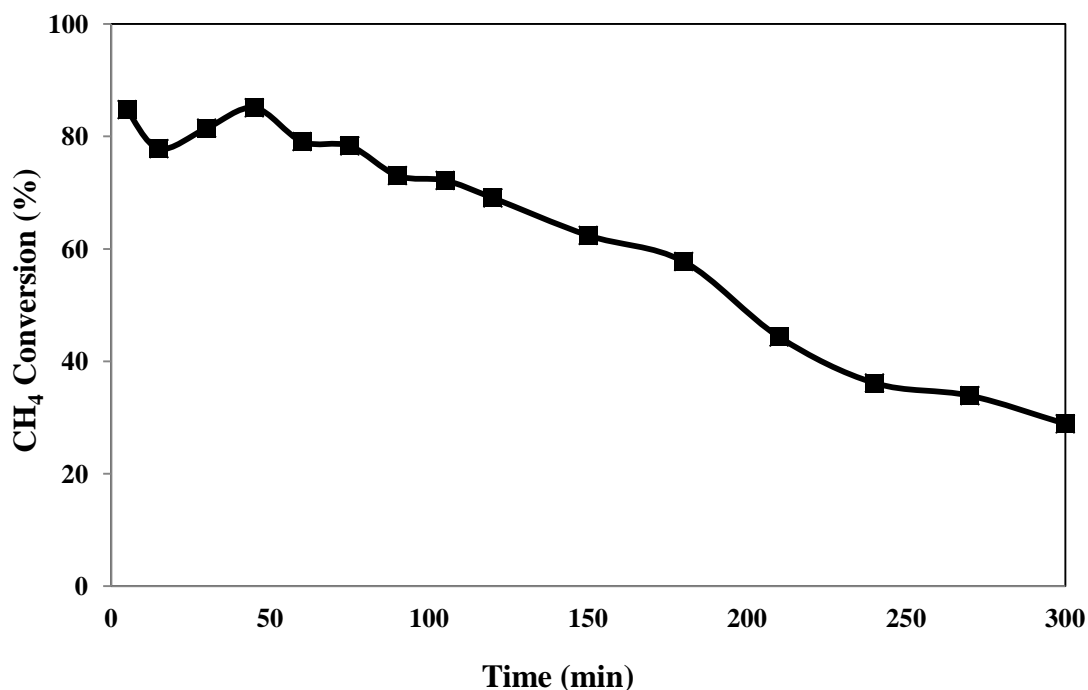

Figure 5.14 Gas product compositions (dry basis) of Type II for the sorption enhanced biogas steam reforming at S/C of 3, CH_4/CO_2 of 1.5, reaction temperature of 600 °C and atmospheric pressure

Figure 5.15 CH_4 conversion of Type II for sorption enhanced biogas steam reforming at S/C of 3, CH_4/CO_2 of 1.5, reaction temperature of 600 °C and atmospheric pressure
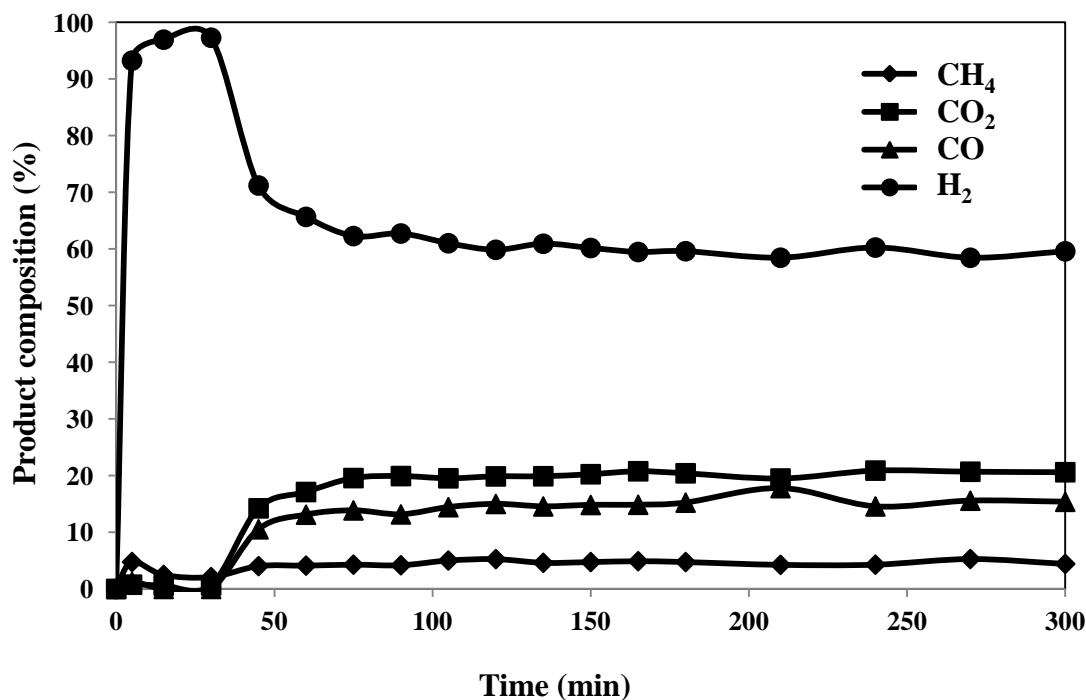
For Type III operation, two beds were packed in the fixed bed reactor. Firstly, 1 g of CaO was packed in the top of fixed bed and secondly, 0.8 g of 12.5 wt.% Ni/Al_2O_3 was mixed with 1 g of CaO and packed into the bottom of fixed bed as shown in Figure 5.8. The results as shown in Figure 5.16 indicated that CO_2 was adsorbed for 45 min and purity of hydrogen as high as 93.8% could be achieved compared to the value of 60% at steady state when CO_2 was no longer adsorbed on the adsorbent. Considering the CH_4 conversion (Figure 5.17), it was reported that only 3% improvement was observed (maximum CH_4 conversions with and without the CO_2 sorption enhancement were 86% and 83%, respectively). It was found that based on this bed arrangement, the sorption enhanced biogas steam reforming did not show significant improvement of CH_4 conversion.

Figure 5.16 Gas product compositions (dry basis) of Type III for sorption enhanced biogas steam reforming at S/C of 3, CH_4/CO_2 of 1.5, reaction temperature of 600 °C and atmospheric pressure
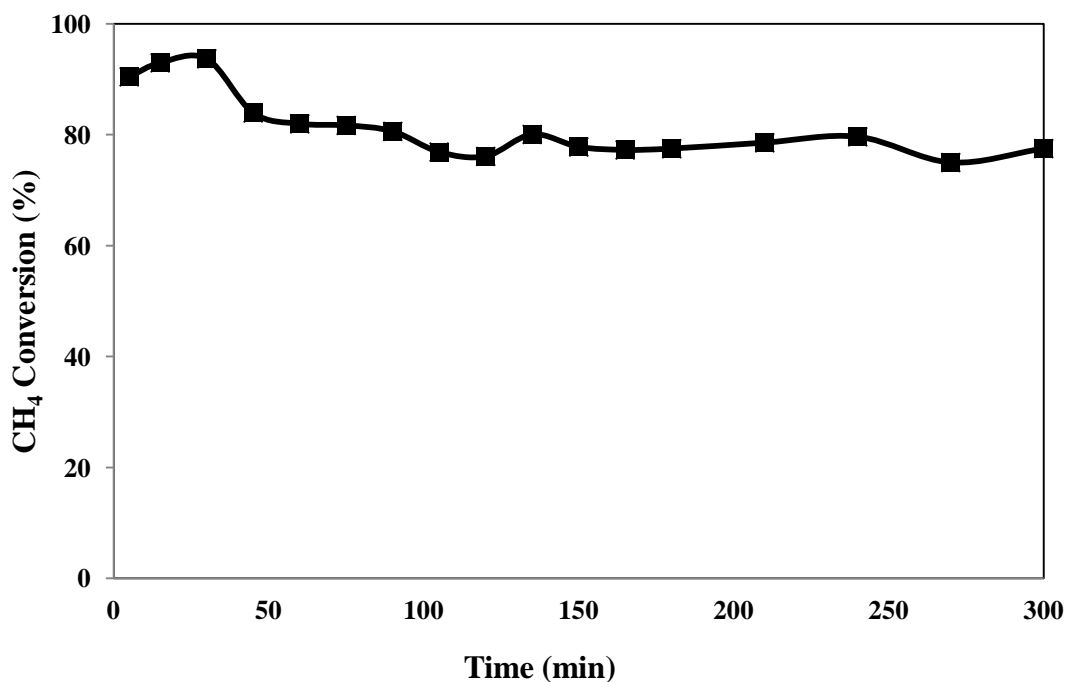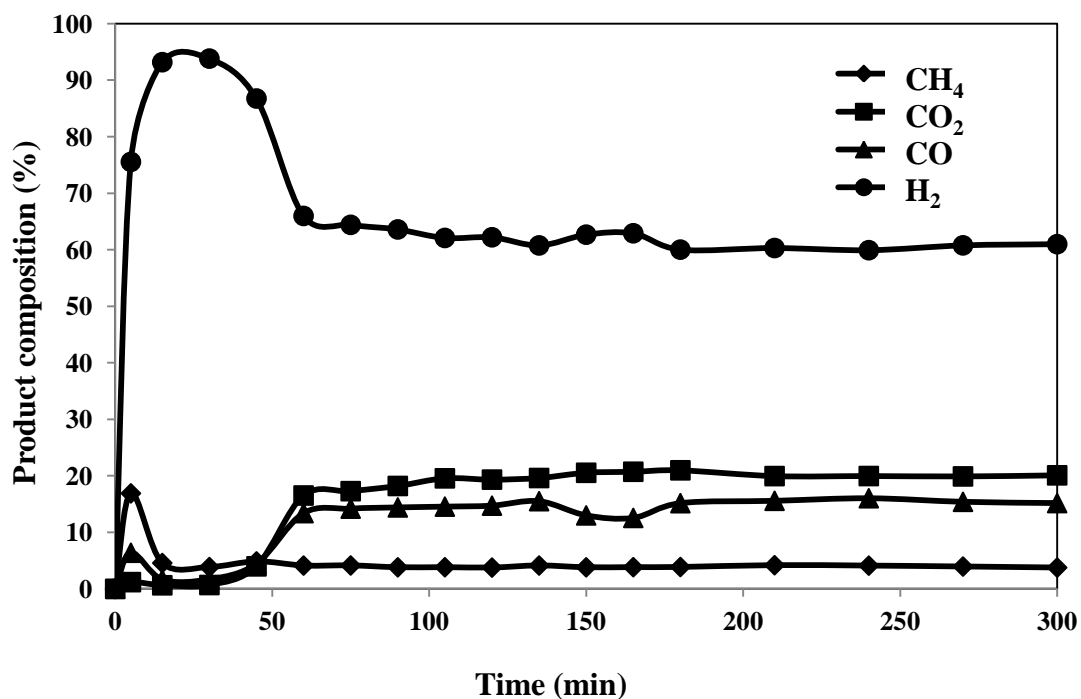

Figure 5.17 CH_4 conversion of Type III for sorption enhanced biogas steam reforming at S/C of 3, CH_4/CO_2 of 1.5, reaction temperature of 600 °C and atmospheric pressure

Table 5.6 Summary of H_2 concentration and CH_4 conversion of different types of bed arrangement for sorption enhanced biogas steam reforming

Type of bed arrangement	H_2 concentration (%)		CH_4 conversion (%)	
	With CO_2 sorption	Without CO_2 sorption	With CO_2 sorption	Without CO_2 sorption
I (a)	-	60	-	82
I (b)	80.7	Deactivation	85.1	Deactivation
II	97.3	60	93.7	80
III	93.8	60	86.1	83

The summary of H_2 concentration and CH_4 conversion for different types of bed arrangement is given in Table 5.6. The suitable bed arrangement for sorption enhanced biogas steam reforming was Type II that used 0.8 g of 12.5 wt.% Ni/Al_2O_3 mixed with 2 g of CaO. In the next study, the same amount of Ni metal was prepared on the same amount of CaO adsorbent in the Type II operation (2 g), resulting in a 5.4 wt.% Ni/CaO catalyst. In Type IV operation, the same amounts of metal and adsorbent as those of Type II were tested. The catalyst (5.4 wt.% Ni/CaO) was mixed with 2 g of SiC and packed into the fixed bed reactor. Then the sorption enhanced biogas steam reforming was carried out. The results as shown in Figures 5.18 and 5.19 indicated that high CH_4 conversion (80-94%) was achieved the operation before 45 min and then CH_4 conversion rapidly decreased (22.7% at 150 min). The purity of hydrogen rapidly decreased from 70.7% at 30 min to 6.1% at 150 min. Similar to the study of Type 1(b) operation, the catalyst deactivation was observed. From Figure 5.20 shows XRD patterns of the fresh and used catalysts. For the used catalyst, the presence of $CaCO_3$ and $Ca(OH)_2$ was observed. The observed results indicate that the deactivation problem was also severe for 5.4 wt.% Ni/CaO even though the content was lower than the 12.5 wt.% Ni/CaO used in the study of Type 1(b).

Figure 5.18 Gas product compositions (dry basis) of Type IV for sorption enhanced biogas steam reforming at S/C of 3, CH_4/CO_2 of 1.5, reaction temperature of 600 °C and atmospheric pressure
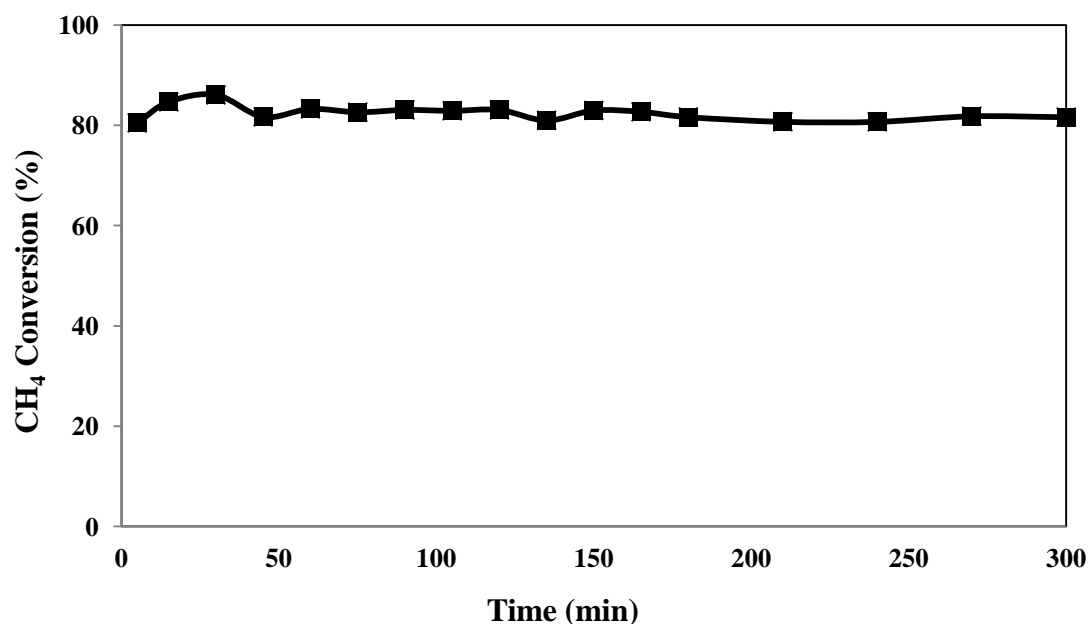

Figure 5.19 CH_4 conversion of Type IV for sorption enhanced biogas steam reforming at S/C of 3, CH_4/CO_2 of 1.5, reaction temperature of 600 °C and atmospheric pressure
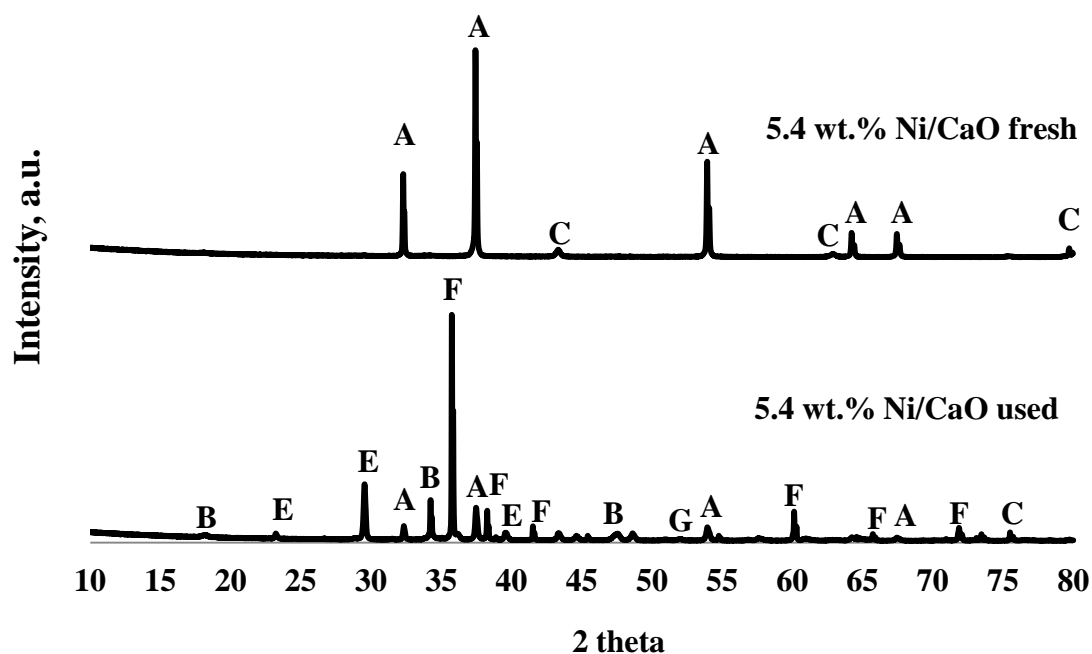
Figure 5.20 XRD patterns of used and fresh catalysts of 5.4 wt.% Ni/CaO (A: CaO, B: Ca(OH)$_2$, C: NiO, D: Al$_2$O$_3$, E: CaCO$_3$, F: SiC and G: Ni)

Although the same amount of Ni in 12.5 wt.% Ni/Al$_2$O$_3$ and 12.5 wt.% Ni/CaO was loaded on 2 g of CaO (suitable amount CaO that used in the bed arrangement of Type II), but the results indicated that deactivation catalyst was observed. Therefore, bed arrangement of Type II was a suitable for sorption enhanced biogas steam reforming. Furthermore, the reaction temperature of 500 °C was tested for the bed arrangement of Type II. The results shown in Figures 5.21 and 5.22 indicated that CH$_4$ conversion was improved to 91.2% when compared with 27% at steady state (without CO$_2$ sorption effect by CaO) and purity of hydrogen was increased to 94.7% when compared with the hydrogen purity of 55% (without CO$_2$ sorption effect).
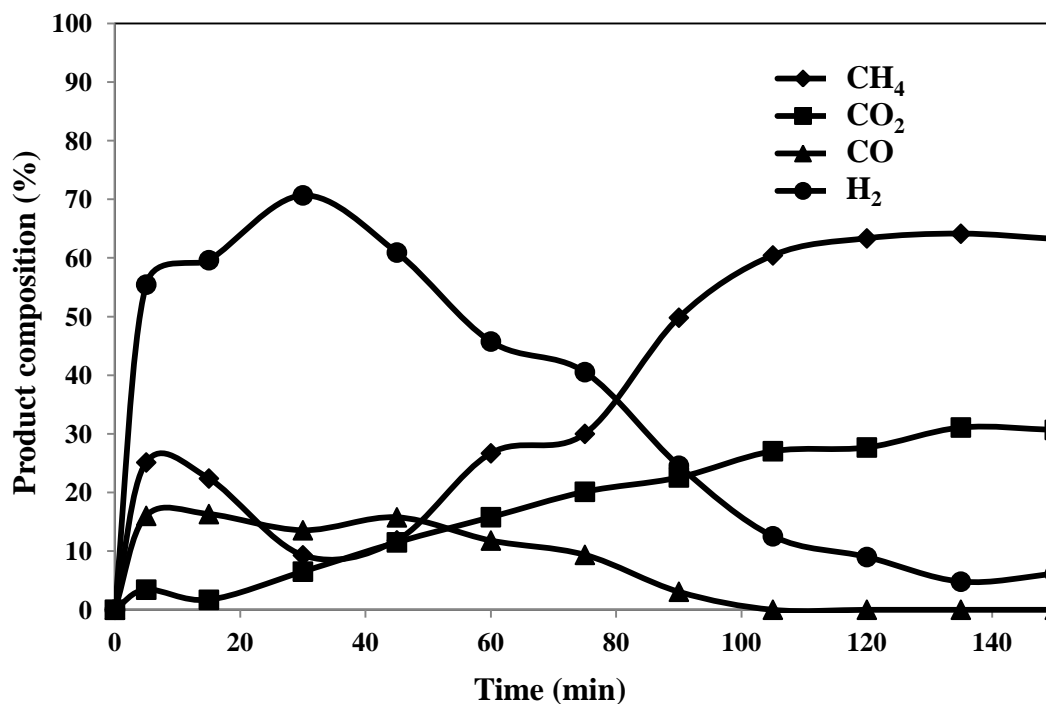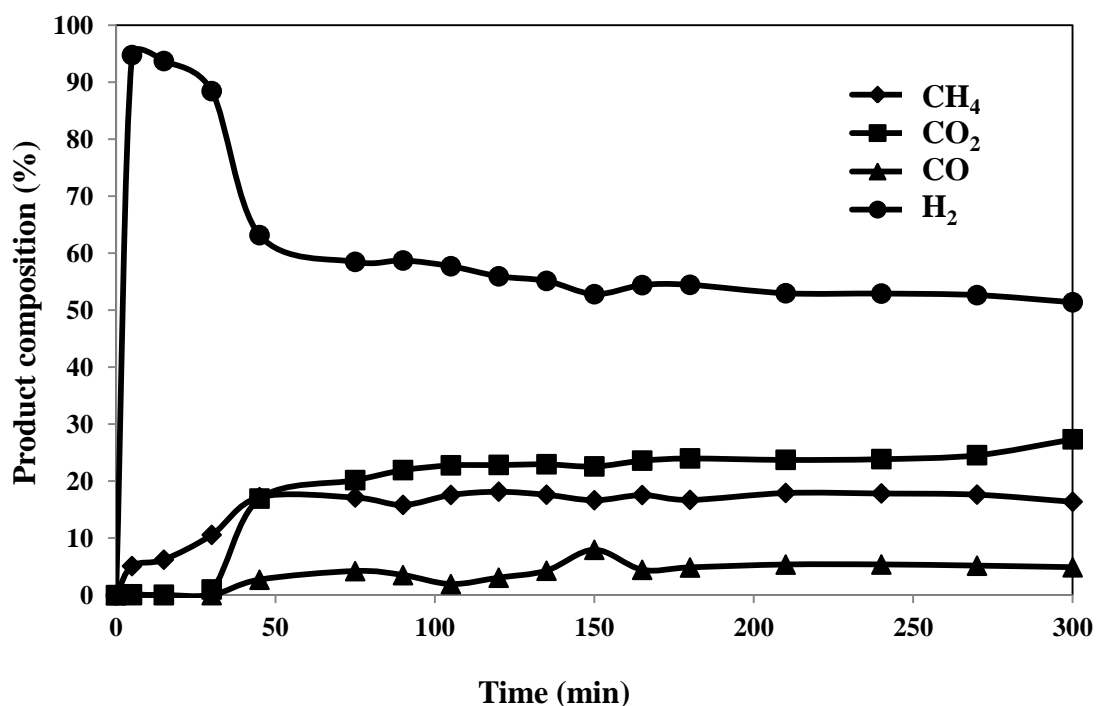
Figure 5.21 Gases product compositions (dry basis) of Type II for sorption enhanced biogas steam reforming at S/C of 3, CH_4/CO_2 of 1.5, reaction temperature of 500 °C and atmospheric pressure
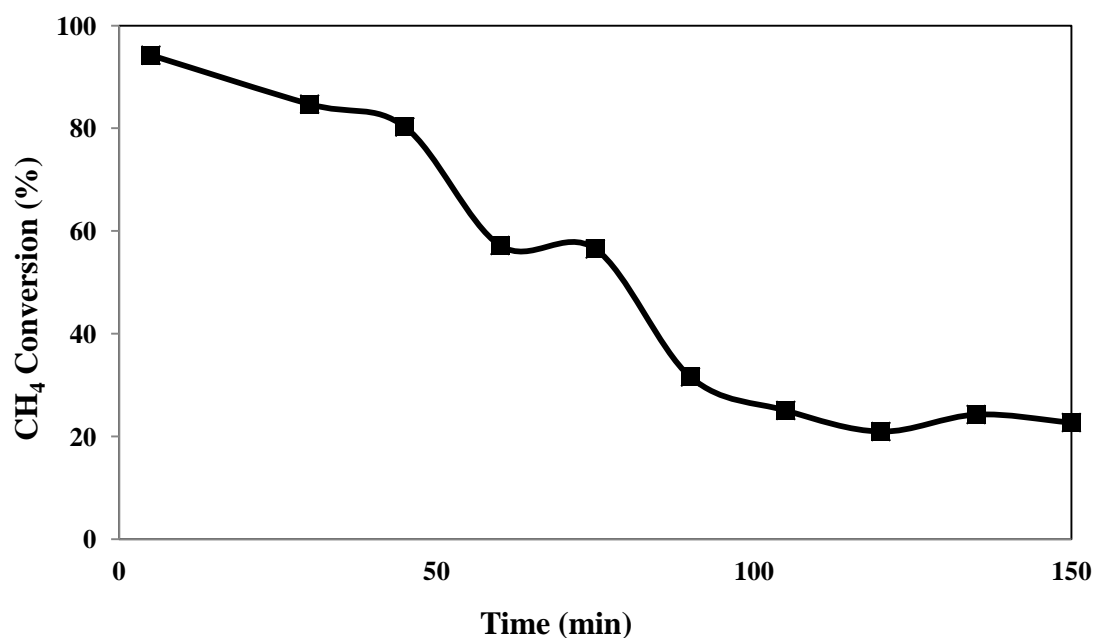

Figure 5.22 CH_4 conversion of Type II for sorption enhanced biogas steam reforming at S/C of 3, CH_4/CO_2 of 1.5, reaction temperature of 500 °C and atmospheric pressure

The effect of reaction temperature for the bed arrangement of Type II at 500 and 600 °C were compared in Figure 5.23. Purity of hydrogen at reaction temperature of 600 °C was higher than purity of hydrogen at reaction temperature of 500 °C, approximately 5-10 % H_2. Furthermore, both of reaction temperatures showed that CH_4 conversion was improved by CO_2 sorption effect (Figure 5.24) and they were increased about 64% and 13% for reaction temperature of 500 and 600 °C, respectively.
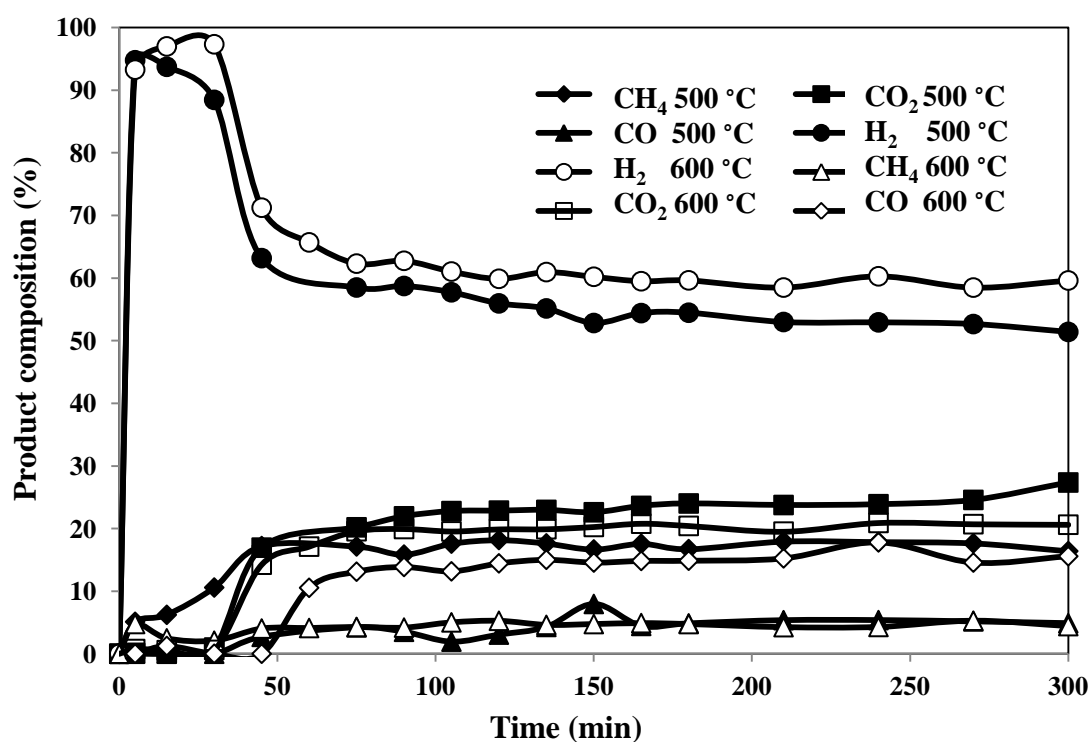
Figure 5.23 Effect of temperatures (500 and 600 °C) of bed arrangement Type II by sorption enhanced biogas steam reforming at S/C of 3, CH_4/CO_2 of 1.5 and atmospheric pressure
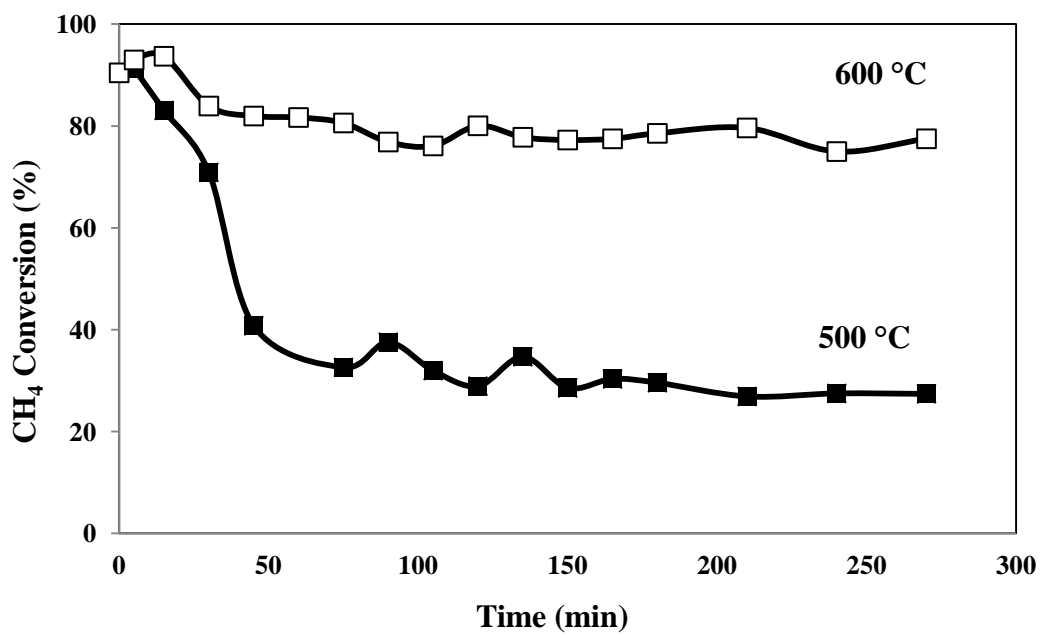
Figure 5.24 CH_4 conversion of Type II for sorption enhanced biogas steam reforming at S/C of 3, CH_4/CO_2 of 1.5 and atmospheric pressure

CHAPTER VI

CONCLUSION AND RECOMMENDATION

6.1 Conclusion

The conclusions from the study of the hydrogen production via sorption enhanced biogas steam reforming process were presented as follows;

1. CO_2 sorption on CaO was tested in order to select the suitable adsorption temperatures. CaO could be reacted with CO_2 and became to $CaCO_3$. The CO_2 sorption capacities were calculated and the results indicated that t_b were 24, 28, 36 and 50 min for temperature of 450, 500, 550 and 600 °C, respectively and CO_2 sorption capacity of 0.1427, 0.1774, 0.2503 and 0.2849 g_{CO2}/g_{CaO} for temperature of 450, 500, 550 and 600 °C, respectively. The highest CO_2 capacity was 0.2849 g_{CO2}/g_{CaO} at adsorption temperature of 600 °C.

2. Different supports of catalyst were tested to determine performance of CO_2 sorption at adsorption temperature of 600 °C including pure CaO, 12.5 wt.% Ni/CaO and 12.5 wt.% Ni/Al_2O_3. The resulted exhibited that no detectable CO_2 sorption by 12.5 wt.% Ni/Al_2O_3. Furthermore, the adsorption capacity of the Ni/CaO was much lower than the pure CaO adsorbent.

3. The effect of the presence of steam in feed was performed by CaO for CO_2 sorption testing at adsorption temperature of 600 °C. The results showed that the CO_2 sorption capacity was increased (0.6724 g_{CO2}/g_{CaO} when steam was presented in the feed) because steam could be reacted with CaO and thus increased its porosity.

4. Four types of bed arrangement were tested for hydrogen production via sorption enhanced biogas steam reforming at S/C of 3, CH_4/CO_2 of 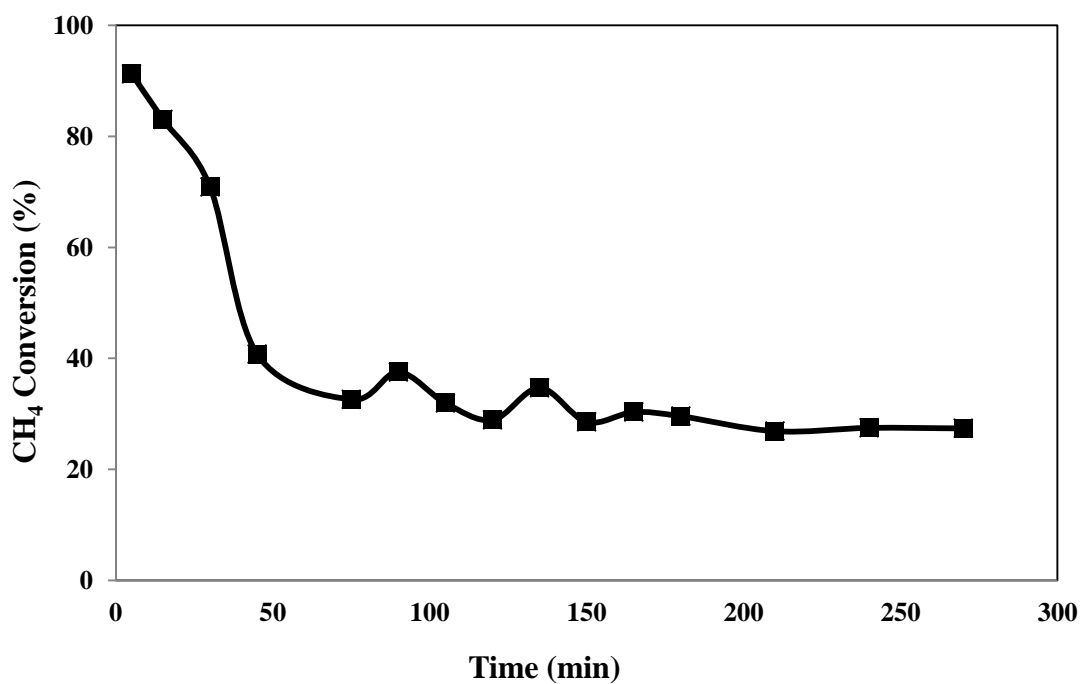1.5, reaction temperature of 600 °C and atmospheric pressure. The results indicated that Type II (catalyst mixed with adsorbent) was the most suitable for the sorption enhanced biogas steam reforming (CH_4 conversion of 93.7% of CO_2 sorption effect when compared with CH_4 conversion of 80% of without CO_2 sorption effect). When the

reaction was carried out at 500 °C, the results showed that high improvement of CH_4 conversion (91.2% CO_2 sorption effect and 27% without CO_2 sorption effect).

5. Both of 12.5 wt.% Ni/CaO and 5.4 wt.% Ni/CaO showed deactivation of catalyst.

6.2 Recommendations

From the experimental results, the recommendation was presented including;

1.   The CO_2 sorption capacity can be increased by increasing its porosity. Steam can be fed before carrying out the reaction because it can increase the porosity of calcium oxide.

2.   Pressure drop is a problem in a fixed bed and it can be solved by making catalyst pellets possible formed by various methods such as spray drying, extrusion process and so on.

REFERENCES

Arias, B., Grasa, G.S., Abanades, J.C. Effect of sorbent hydration on the average activity of CaO in a Ca-looping system. Chemical Engineering Journal and the Biochemical Engineering Journal. 163 (2010): 324–330.

Avraam, D.G., Halkides, T.I., Liguras, D.K., Bereketidou, O.A., Goula, M.A. An experimental and theoretical approach for the biogas steam reforming reaction. International Journal of Hydrogen Energy. 35 (2010): 9818–9827.

Balasubramanian, B., Ortiz, L.A., Kaytakoglu, S., Harrison, P.D. Hydrogen from methane in a single-step process. Chemical Engineering Science. 54 (1999): 3543–3552.

Barelli, L., Bidini, G., Gallorini, F., Servili, S. Hydrogen production through sorption-enhanced steam methane reforming and membrane technology: A review. Energy. 33 (2008): 554–570.

Barroso-Quiroga, M.M., Castro-Luna, A.E. Catalytic activity and effect of modifiers on Ni-based catalysts for the dry reforming of methane. International Journal of Hydrogen Energy. 35 (2010): 6052–6056.

Basile, A., Parmaliana, A., Tosti, S., Lulianelli, A., Gallucci, F., Espro, C., Spooren, J. Hydrogen production by methanol steam reforming carried out in membrane reactor on Cu/Zn/Mg-based catalyst. Catalysis Today. 137 (2008): 17–22.

Blamey, J., Lu, Y.D., Fennell, S.P., Anthony, E.J. Reactivation of CaO-based sorbents for CO_2 capture: Mechanism for the carbonation of $Ca(OH)_2$. Industrial & Engineering Chemistry Research. 50 (2011): 10329–10334.

Bouarab, R., Akdim, O., Auroux, A., Cherifi, O., Mirodatos, C. Effect of MgO additive on catalytic properties of Co/SiO_2 in the dry reforming of methane. Applied Catalysis A: General. 264 (2004): 161–168.

Carrero, A., Calles, J.A., Vizcaíno, A.J. Effect of Mg and Ca addition on coke deposition over $Cu–Ni/SiO_2$ catalysts for ethanol steam reforming. Chemical Engineering Journal. 163 (2010): 395–402.

Carrieri, D., Ananyev, G., Costas A.M.G., Bryant D.A., Dismukes G.C. Renewable hydrogen production by cyanobacteria: Nickel requirements for optimal

hydrogenase activity. International Journal of Hydrogen Energy. 33 (2008): 2014–2022.

Casanovas, A., Leitenburg, C., Trovarelli, A., Llorca, J. Ethanol steam reforming and water gas shift reaction over Co–Mn/ZnO catalysts. Chemical Engineering Journal. 154 (2009): 267–273.

Chanburanasiri, N., Ribeiro, M.A., Rodrigues, E.A., Arpornwichanop, A., Laosiripojana, N., Praserthdam, P., Assabumrungrat, S. Hydrogen production via sorption enhanced steam methane reforming process using Ni/CaO multifunctional catalyst. Industrial & Engineering Chemistry Research. 50 (2011): 13662–13671.

Cheng, J., Huang, W. Effect of cobalt (nickel) content on the catalytic performance of molybdenum carbides in dry-methane reforming. Fuel Processing Technology. 91 (2010): 185–193.

Dholam, R., Patel, N., Adami, M., Miotello, A. Hydrogen production by photocatalytic water-splitting using Cr- or Fe-doped TiO_2 composite thin films photocatalyst. International Journal of Hydrogen Energy. 34 (2009): 5337–5346.

Dholam, R., Patel, N., Miotello A. Efficient H_2 production by water-splitting using indiumetin-oxide/V-doped TiO_2 multilayer thin film photocatalyst. International Journal of Hydrogen Energy. xxx (2011): 1–10.

Djaidja, A., Libs, S., Kiennemann, A., Barama, A. Characterization and activity in dry reforming of methane on NiMg/Al and Ni/MgO catalysts. Catalysis Today. 113 (2006): 194–200.

Dong, W., Roh, H., Jun, K., Park, S., Oh, Y. Methane reforming over Ni/Ce-ZrO_2 catalysts: effect of nickel content. Applied Catalysis A: General. 226 (2002): 63–72.

Dou, B., Dupont, V., Rickett, G., Blakeman, N., Williams T.P., Chen, H., Ding, Y., Ghadiri, M. Hydrogen production by sorption-enhanced steam reforming of glycerol. Bioresource Technology. 100 (2009): 3540–3547.

Essaki, K., Muramatsu, T., Kato, M. Effect of equilibrium shift by using lithium silicate pellets in methane steam reforming. International Journal of Hydrogen Energy. 33 (2008): 4555–4559.

Essaki, K., Muramatsu, Y., Kato, M. Effect of equilibrium-shift in the case of using lithium silicate pellets in ethanol steam reforming. International Journal of Hydrogen Energy. 33 (2008): 6612–6618.

Frusteri, F., Arena, F., Calogero, G., Torre, T., Parmaliana, A. Potassium-enhanced stability of Ni/MgO catalysts in the dry reforming of methane. Catalysis Communications. 2 (2001): 49–56.

Hildenbrand, N., Readman, J., Dahl, I.M., Blom, R. Sorbent enhanced steam reforming (SESR) of methane using dolomite as internal carbon dioxide absorbent: Limitations due to $Ca(OH)_2$ formation. Applied Catalysis A: General. 303 (2006): 131–137.

Hong, X., Ren, S. Selective hydrogen production from methanol oxidative steam reforming over Zn–Cr catalysts with or without Cu loading. International Journal of Hydrogen Energy. 33 (2008): 700–708.

Huang, T.J., Chen, H.M. Hydrogen production via steam reforming of methanol over $Cu/(Ce,Gd)O_{2-x}$ catalysts. International Journal of Hydrogen Energy. 35 (2010): 6218–6226.

Ishida, M., Yamamoto, T., Ohba, T. Experimental results of chemical-looping combustion with $NiO/NiAl_2O_4$ particle circulation at 1200 °C. Energy Conversion and Management. 43 (2002): 1469–1478.

Johnsen, K., Ryu, H.J., Grace, J.R., Lim, C.J. Sorption-enhanced steam reforming of methane in a fluidized bed reactorwith dolomite as CO_2-acceptor. Chemical Engineering Science. 61 (2006): 1191–1198.

Juan-Juan, J., Román-Martĭnez, M.C., Illán-Gómez, M.J. Effect of potassium content in the activity of K-promoted Ni/Al_2O_3 catalysts for the dry reforming of methane. Applied Catalysis A: General. 301 (2006): 9–15.

Kalinci, Y., Hepbasli, A., Dincer, I. Biomass-based hydrogen production: A review and analysis. International Journal of Hydrogen Energy. 34 (2009): 8799–8817.

Kambolis, A., Matralis, H., Trovarelli, A., Papadopoulou, Ch. Ni/CeO_2-ZrO_2 catalysts for the dry reforming of methane. Applied Catalysis A: General. 377 (2010): 16–26.

Kolbitsch, P., Pfeifer, C., Hofbauer, H. Catalytic steam reforming of model biogas. Fuel. 87 (2008): 701–706.

Laoun, B. Thermodynamics aspect of high pressure hydrogen production by water electrolysis. Revue des Energies Renouvelables. 10 (2007): 435–444.

Lertwittayanon, K., Atong, D., Aungkavattana, P., Wasanapiarnpong, T., Wada, S., Sricharoenchaikul, V. Effect of CaO-ZrO$_2$ addition to Ni supported on γ-Al$_2$O$_3$ by sequential impregnation in steam methane reforming. International Journal of Hydrogen Energy. 35 (2010): 12277–12285.

Li, H., Wang, J. Study on CO$_2$ reforming of methane to syngas over Al$_2$O$_3$–ZrO$_2$ supported Ni catalysts prepared via a direct sol–gel process. Chemical Engineering Science. 59 (2004): 4861–4867.

Li, H., Xu, H., Wang, J. Methane reforming with CO$_2$ to syngas over CeO$_2$-promoted Ni/Al$_2$O$_3$-ZrO$_2$ catalysts prepared via a direct sol-gel process. Journal of Natural Gas Chemistry. 20 (2011): 1–8.

Liu, Z., Pesic, B., Raja, K.S., Rangaraju, R.R., Misra, M. Hydrogen generation under sunlight by self ordered TiO$_2$ nanotube arrays. International Journal of Hydrogen Energy. 34 (2009): 3250–3257.

Maluf, S.S., Assaf, E.M. Ni catalysts with Mo promoter for methane steam reforming. Fuel. 88 (2009): 1547–1553.

Martavaltzi, S.C., Lemonidou, A.A. Hydrogen production via sorption enhanced reforming of methane: Development of a novel hybrid material-reforming catalyst and CO$_2$ sorbent. Chemical Engineering Science. 65 (2010): 4134–4140.

Matsumura, Y., Nakamori, T. Steam reforming of methane over nickel catalysts at low reaction temperature. Applied Catalysis A: General. 258 (2004): 107–114.

Moon, S.C., Mametsuka, H., Tabata, S., Suzuki, E. Photocatalytic production of hydrogen from water using TiO$_2$ and B/TiO$_2$. Catalysis Today. 58 (2000): 125–132.

Muradov, N., Smith, F., T-Raissi, A. Hydrogen production by catalytic processing of renewable methane-rich gases. International Journal of Hydrogen Energy. 33 (2008): 2023–2035.

Ochoa-Fernández, E., Haugen, G., Zhao, T., Rønning, M., Aartun, I., Børresen, B., Rytter, E., Rønnekleiv, M., Chen, D. Process design simulation of H_2 production by sorption enhanced steam methane reforming: evaluation of potential CO_2 acceptors. Green Chemistry. 9 (2007): 654–662.

Oliveira, L. G. E., Grande, A. C., Rodrigues, E. A. CO_2 sorption on hydrotalcite and alkali-modified (K and Cs) hydrotalcites at high temperatures. Separation and Purification Technology. 62 (2008): 137–147.

Peppley, B.A., Amphlett, J.C., Kearns, L.M., Mann, R.F. Methanol steam reforming on $Cu/ZnO/Al_2O_3$. Part 1: the reaction network. Applied Catalysis A: General. 179 (1999): 21–29.

Pistonesi, C., Juan, A., Irigoyen, B., Amadeo, N. Theoretical and experimental study of methane steam reforming reactions over nickel catalyst. Applied Surface Science. 253 (2007): 4427–4437.

Pompeo, F., Gazzoli, D., Nichio, N.N. Stability improvements of Ni/α-Al_2O_3 catalysts to obtain hydrogen from methane reforming. International Journal of Hydrogen Energy. 34 (2009): 2260–2268.

Reijers, Th. J. H., Valster-Schiermeier, E. A. S., Cobden, D. P., Brink, W. R. Hydrotalcite as CO_2 Sorbent for Sorption-Enhanced Steam Reforming of Methane. Industrial & Engineering Chemistry Research. 45 (2006): 2522–2530.

Roh, H., Jun, K., Dong, W., Chang, J., Park, S., Joe, Y. Highly active and stable Ni/Ce–ZrO_2 catalyst for H_2 production from methane. Journal of Molecular Catalysis A: Chemical. 181 (2002): 137–142.

San-José-Alonso, D., Juan-Juan, J., Illán-Gómez, M.J., Román-Martĭnez, M.C. Ni, Co and bimetallic Ni–Co catalysts for the dry reforming of methane. Applied Catalysis A: General. 371 (2009): 54–59.

Silva, L.A., Müller, L.I. Hydrogen production by sorption enhanced steam reforming of oxygenated hydrocarbons (ethanol, glycerol, n-butanol and methanol): Thermodynamic modelling. International Journal of Hydrogen Energy. 36 (2011): 2057–2075.

Solieman, A.A.A., Dijkstra J.W., Haije W.G., Cobden P.D., van den Brink R.W. Calcium oxide for CO_2 capture: Operational window and efficiency penalty in

sorption-enhanced steam methane reforming. International Journal of Greenhouse Gas Control. 3 (2009): 393–400.

Sreethawong, T., Junbua, C., Chavadej, S. Photocatalytic H_2 production from water splitting under visible light irradiation using Eosin Y-sensitized mesoporous-assembled Pt/TiO_2 nanocrystal photocatalyst. Journal of Power Sources. 190 (2009): 513–524.

Sultana, K.S., Chen, D. Enhanced hydrogen production by in situ CO_2 removal on CaCeZrOx nanocrystals. Catalyst Today. 171 (2011): 43–51.

Sun, P., Grace, J.R., Lim, C.J., Anthony, E.J. Investigation of attempts to improve cyclic CO_2 capture by sorbent hydration and modification. Industrial & Engineering Chemistry Research. 47 (2008): 2024–2032.

Tiwari, G.N., Mishra, R.K., Solanki, S.C. Photovoltaic modules and their applications: A review on thermal modelling. Applied Energy. 88 (2011): 2287–2304.

Urasaki, K., Sekine, Y., Kawabe, S., Kikuchi, E., Matsukata, M. Catalytic activities and coking resistance of Ni/perovskites in steam reforming of methane. Applied Catalysis A: General. 286 (2005): 23–29.

Wang, X., Wang, N., Wang, L. Hydrogen production by sorption enhanced steam reforming of propane: A thermodynamic investigation. International Journal of Hydrogen Energy. 36 (2011): 466–472.

Westermann, P., Jorgensen, B., Lange, L., Ahring, B.K., Christensen, C.H. Maximizing renewable hydrogen production frombiomass in a bio/catalytic refinery. International Journal of Hydrogen Energy. 32 (2007): 4135–4141.

Youn, M.H., Seo, J.G., Song, I.K. Hydrogen production by auto-thermal reforming of ethanol over nickel catalyst supported on metal oxide-stabilized zirconia. International Journal of Hydrogen Energy. 35 (2010): 3490–3498.

Zhai, X., Ding, S., Liu, Z., Jin, Y., Cheng, Y. Catalytic performance of Ni catalysts for steam reforming of methane at high space velocity. International Journal of Hydrogen Energy. 36 (2011): 482–489.

Zhang, Q.H., Li, Y., Xu, B.Q. Reforming of methane and coalbed methane over nanocomposite Ni/ZrO_2 catalyst. Catalyst Today. 98 (2004): 601–605.

APPENDICES
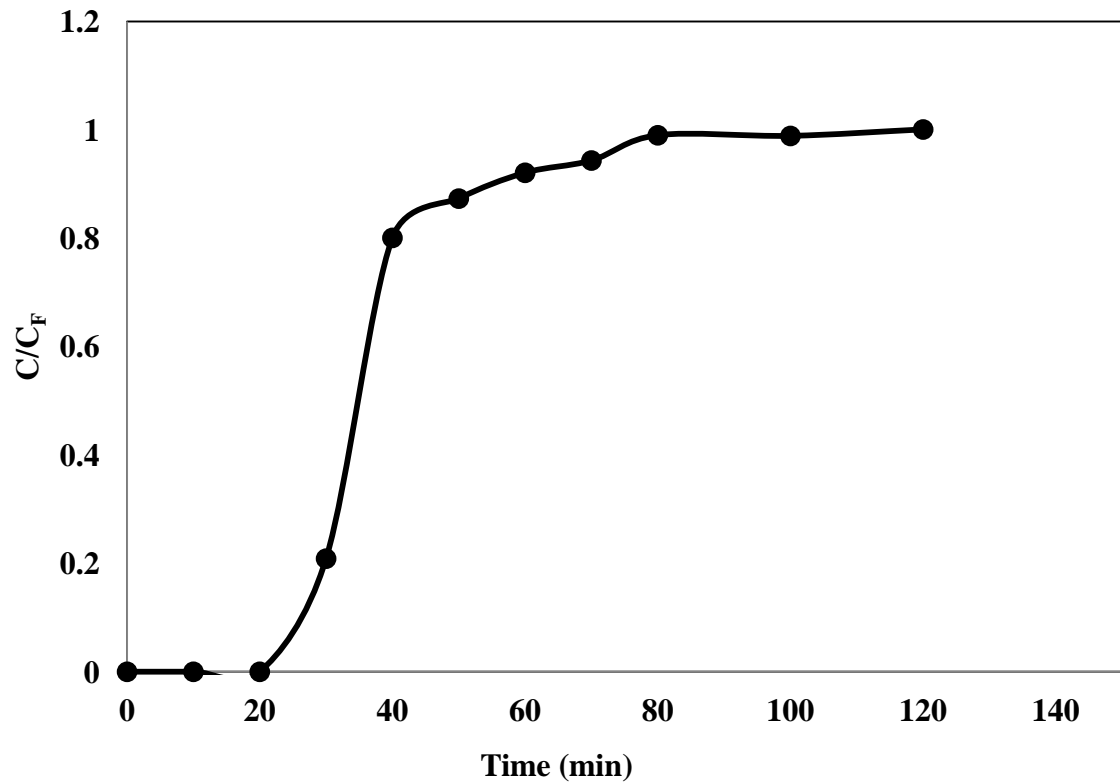
APPENDIX A

CALCULATIONS OF ADSORPTION CAPACITY

Figure A.1 CO_2 sorption by CaO at adsorption temperature of 450 °C, atmospheric pressure and 8% CO_2 in N_2 feed.

Adsorption capacity of adsorbent

W_{sat} = amount of CO_2 (g) divided by amount of adsorbent (g)

$$= \frac{F_A \times above\ graph\ area}{amount\ of\ adsorbent} \qquad \dots (A.1)$$

1. Find rate of feed

$$F_A = u_0 c_o M$$

Where $F_A = rate\ of\ feed\ \left(\frac{g}{min}\right)$

$$u_0 = velocity\ of\ feed\ \left(\frac{cm^3}{min}\right)$$

$$c_0 = concentration\ of\ feed\ \left(\frac{mol}{cm^3}\right)$$

$$M = molecular\ weight\ of\ feed\ \left(\frac{g}{mol}\right)$$

Therefore; $\quad \mathbf{F_A} = \left(50\ \frac{cm^3}{min}\right) \times (3.43 \times 10^{-6})\frac{mol}{cm^3} \times (44\ \frac{g}{mol})$

$$= 0.00755\ \frac{g}{min}$$

2. Find above graph area

$$Above\ graph\ area\ = \int_0^{120} \left(1 - \frac{C}{C_0}\right)dt$$

$$= 38\ (min)$$

Substitute 1-2 into equation A.1

$$W_{sat} = \frac{0.00755\ \left(\frac{g}{min}\right) \times 38\ (min)}{2.0113\ (g)}$$

$$W_{sat} = 0.1427\ \left(\frac{g_{CO_2}}{g_{CaO}}\right)$$

Therefore, 1 g of CaO can adsorb 0.1427 g of CO_2 at 450 °C, atmospheric pressure and 8% CO_2 in N_2 feed.

APPENDIX B

CALCULATIONS FOR SORPTION ENHANCED BIOGAS STEAM REFORMING PROCESS

Biogas steam reforming process is a process whose main reactions are methane steam reforming (Equation B.1) and dry methane reforming (Equation B.3). Moreover, the side reaction is water gas shift reaction (Equation B.2). For this study, the experiments were performed using excess steam at S/C of 3. Calculations for methane/carbon dioxide ratio, steam/carbon ratio and methane conversion equations are shown in Equations B.4-B.6, respectively.

$$CH_4 + H_2O \rightarrow 3H_2 + CO \qquad \Delta H^0_{298} = +206 \text{ kJ/mol} \qquad \dots \text{(B.1)}$$

$$CO + H_2O \rightarrow H_2 + CO_2 \qquad \Delta H^0_{298} = -41.1 \text{ kJ/mol} \qquad \dots \text{(B.2)}$$

$$CH_4 + CO_2 \rightarrow CO + H_2 \qquad \Delta H^0_{298} = +247 \text{ kJ/mol} \qquad \dots \text{(B.3)}$$

Methane/carbon dioxide ratio

$$CH_4/CO_2 = \frac{\% \text{ composition of methane}}{\% \text{ composition of carbon dioxide}} \qquad \dots \text{(B.4)}$$

$$= \frac{60 \ (\%)}{40 \ (\%)}$$

$$= 1.5$$

Steam/carbon molar ratio:

$$S/C = \frac{Y_{H_2O,in}}{Y_{CH_4,in}} \qquad \text{(mol/mol)} \qquad \dots \text{(B.5)}$$

$$= \frac{3 \ mole}{1 \ mole}$$

$$= 3$$

The conversions of substance CH_4:

$$Conversion\ (CH_4) = \frac{F_{CH4,in} - F_{CH4,out}}{F_{CH4,in}} \times (100\%) \qquad \ldots (B.6)$$

APPENDIX C

CALIBRATION CURVE

Calibration curve is done from gas chromatography (GC-8A) equipped with two column that are Molecular Sieve and Poraplot column. Table C.1 shows the operating conditions for gas chromatography. The gas standard is injected to gas chromatography at different concentrations and we get peak area from GC for each concentration. Then, plot graph between peak area of gas chromatography and mole of gas that we inject into gas chromatography. Calibration curves are shown in Figures C.1-C.5 for CO_2, H_2, N_2, CH_4 and CO, respectively.

Table C.1 Operating conditions for gas chromatography

Gas Chromatography	Shimadzu GC-8A	
Detector	TCD	
Column	Molecular sieve 5A	Porapak-Q
- Column material	SUS	SUS
- Length (m)	2	2
- Outer diameter (mm)	4	4
- Inner diameter (mm)	3	3
- Mesh range	60/80	60/80
- Maximum temperature (˚C)	350	350
Carrier gas	Ar (99.999%)	Ar (99.999%)
Column temperature		
- initial (˚C)	50	50
- final (˚C)	50	50
Injector temperature (˚C)	70	70
Detector temperature (˚C)	100	100
Current (mA)	70	70
Analyzed gas	N_2, H_2, CO, CH_4	CO_2

Figure C.1 Calibration curve of CO_2

$y = 1.1558E\text{-}10x$
$R^2 = 9.9981E\text{-}01$
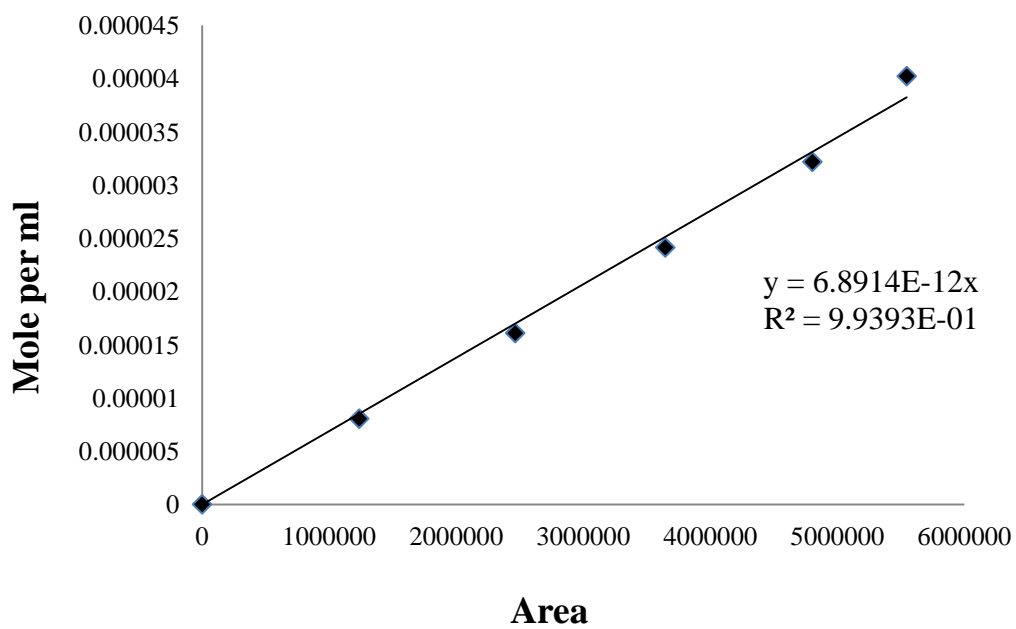
Figure C.2 Calibration curve of H_2

$y = 6.8914E\text{-}12x$
$R^2 = 9.9393E\text{-}01$
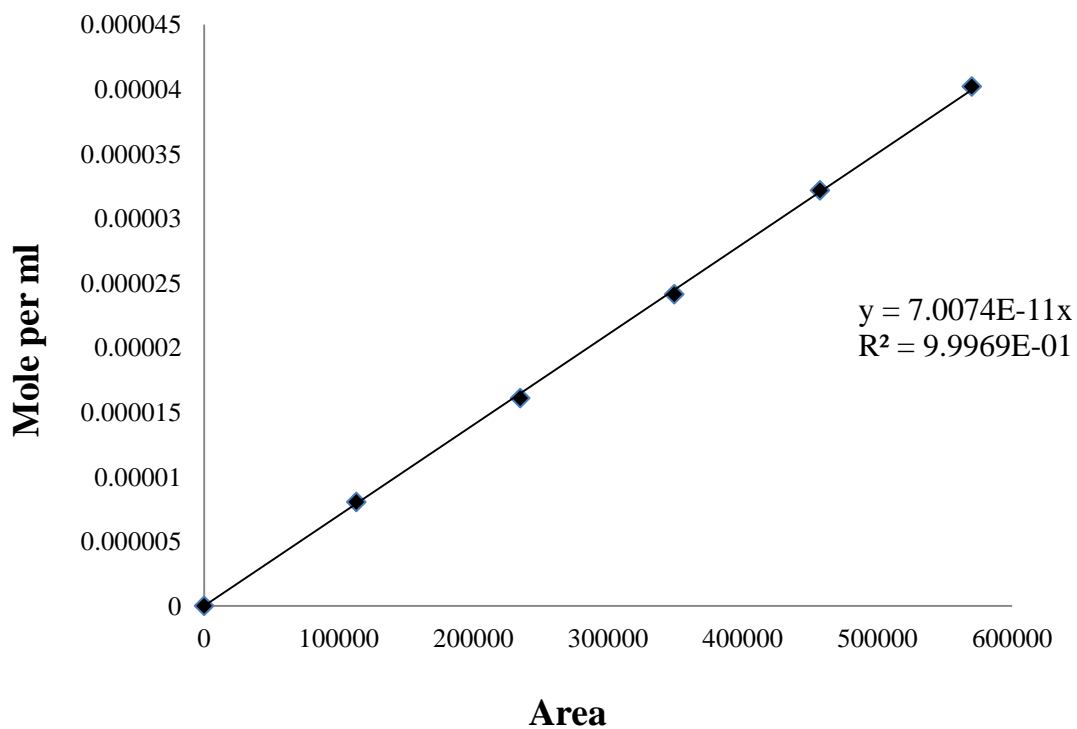
Figure C.3 Calibration curve of N_2

$y = 7.0074E\text{-}11x$
$R^2 = 9.9969E\text{-}01$

Figure C.4 Calibration curve of CH_4

$y = 2.6980E\text{-}11x$
$R^2 = 9.9895E\text{-}01$

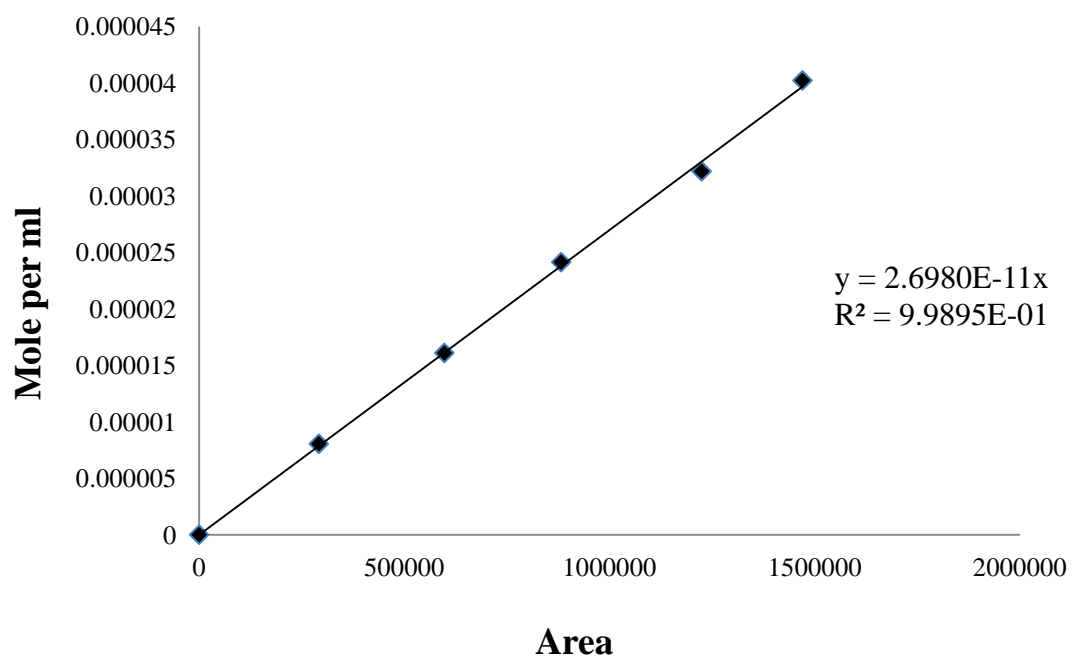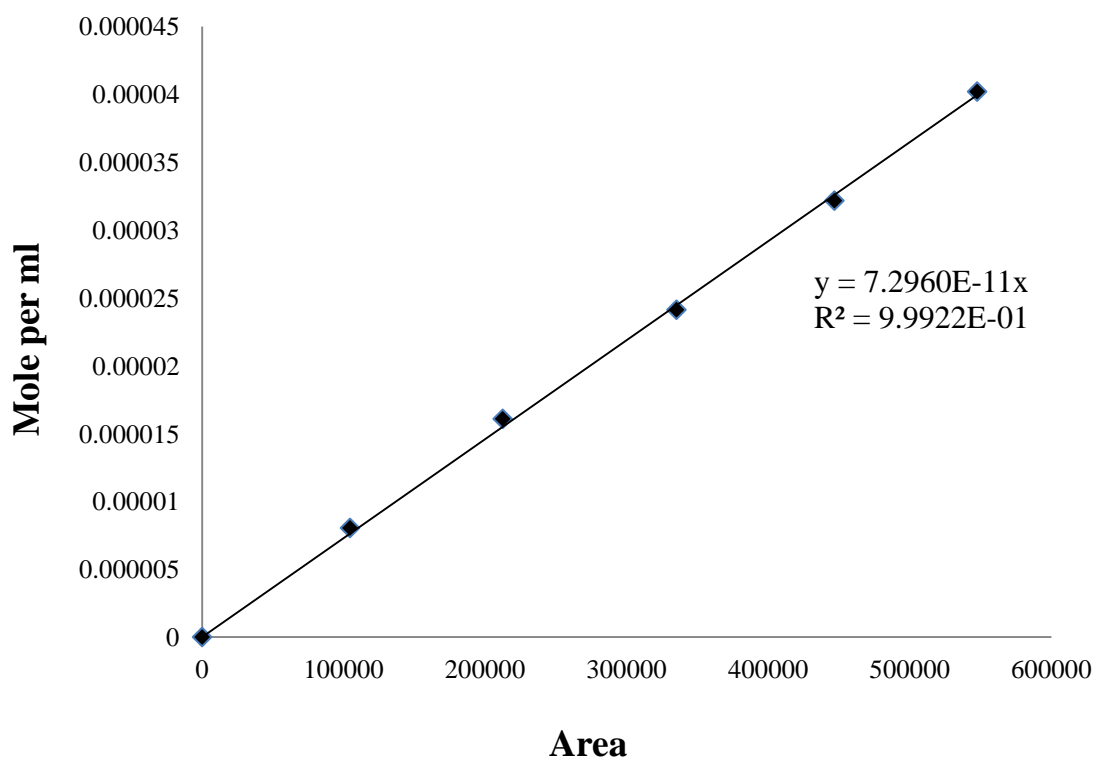**Figure C.5** Calibration curve of CO

VITA

Mr. Janewit Phromprasit was born in Surin province, Thailand, on September 7, 1987. He finished high school from Pibulwittayalai School, Lob Buri, Thailand, 2006. He received his Bachelor's Degree of Chemical Engineering, Thammasat University, Thailand, 2010. He has been studying Master's Degree of Chemical Engineering, Chulalongkorn University, Thailand, 2012.